The telomere binding protein Pot1 maintains haematopoietic stem cell activity with age

Kentaro Hosokawa[1, 2], Ben D. MacArthur[3], Yoshiko Matsumoto Ikushima[2,4], Hirofumi Toyama[2], Yoshikazu Masuhiro[5], Shigemasa Hanazawa[5], Toshio Suda[2, 6, 7], Fumio Arai[1, 2, 7]

[1]Department of Stem Cell Biology and Medicine, Graduate School of Medical Sciences, Kyushu University, 3-1-1 Maidashi, Higashi-ku, Fukuoka 812-8582, Japan

[2]Department of Cell Differentiation, The Sakaguchi Laboratory of Developmental Biology, School of Medicine, Keio University, 35 Shinanomachi, Shinjuku-ku, Tokyo 160-8582, Japan

[3]Centre for Human Development, Stem Cells and Regeneration, Faculty of Medicine, University of Southampton, University Road, Southampton SO17 1BJ, United Kingdom

[4]National Center for Global Health and Medicine, 1-21-1 Toyama, Shinjuku-ku, Tokyo 162-8655, Japan

[5]Laboratory of Molecular and Cellular Physiology, Department of Applied Biological Sciences, College of Bioresource Sciences, Nihon University, Fujisawa City, Kanagawa 252-0880, Japan

[6]Cancer Science Institute of Singapore, National University of Singapore, Singapore 117599

[7]Contact Information: Correspondence should be addressed to T.S. (sudato@keio.jp) and F.A. (farai@scr.med.kyushu-u.ac.jp)

Abstract

Repeated cell divisions and aging impair stem cell function. However, the mechanisms by which this occurs are not fully understood. Here we show that protection of telomeres 1A (Pot1a), a component of the Shelterin complex that protects telomeres, improves haematopoietic stem cell (HSC) activity during aging. Pot1a is highly expressed in young HSCs but declines with age. In mouse HSCs, Pot1a knockdown increases DNA damage response (DDR) and inhibits self-renewal. Conversely, Pot1a overexpression or treatment with POT1a protein prevents DDR, maintained self-renewal activity and rejuvenated aged HSCs upon *ex vivo* culture. Moreover, treatment of HSCs with exogenous Pot1a inhibits the production of reactive oxygen species, suggesting a non-telomeric role for Pot1a in HSC maintenance. Consistent with these results, treatment with exogenous human POT1 protein maintains human HSC activity in culture. Collectively, these results show that Pot1a/POT1 sustains HSC activity and can be used to expand HSC numbers *ex vivo*.

Introduction

Appropriate regulation of haematopoietic stem cell (HSC) self-renewal is critical for the maintenance of life long hematopoiesis. However, long-term repeated cell divisions induce the accumulation of DNA damage, which, along with replication stress, significantly compromises HSC function[1-6]. This sensitivity to stress-induced DNA-damage is a primary obstacle to establishing robust protocols for the *ex vivo* expansion of functional HSCs. Telomeres are particularly sensitive to such damage because they are fragile sites in the genome[3, 7, 8]. Since HSCs lose telomeric DNA with each cell division[9], which ultimately limits their replicative potential[10], HSCs therefore require a protective mechanism to prevent DNA damage response (DDR) at telomeres in order to maintain their function.

The shelterin complex – which contains 6 subunit proteins, TRF1, TRF2, POT1, TIN2, TPP1, and RAP1 – has a crucial role in the regulation of telomere length and loop structure, as well as in the protection of telomeres from ataxia telangiectasia-mutated (ATM) and ATM- and RAD3-related (ATR) dependent DDR signaling pathways[11, 12]. Protection of telomeres 1 (POT1) binds to telomeric single-stranded DNA (ssDNA) through its oligonucleotide/oligosaccharide-binding fold domains (OB domains)[13, 14] and thereby prevents ATR signaling by blocking replication protein A (RPA), the ssDNA binding protein that activates the ATR pathway[15]. Furthermore, POT1 can also bind to sub-telomeric and non-telomeric DNA through its OB1 domain, which recognizes an OB1-biding motif (TTAGG) and a non-telomeric motif, suggesting further non-telomeric functions for POT1 related to gene transcription, replication, or repair[16].

Human shelterin contains a single POT1 protein, whereas the mouse genome has two *POT1* orthologs, *Pot1a* and *Pot1b*, which have different functions at telomeres[17]. Pot1a is

required for the repression of DDR at telomeres[17, 18]. In contrast, Pot1b is involved in the maintenance of telomere terminus structure[17, 19, 20]. Commensurate with these different roles, *Pot1a* knockout (KO) mice have early embryonic lethality, whereas *Pot1b* KO mice remain alive and fertile and exhibit a dyskeratosis congenita-like phenotype when generated in a telomerase-haploinsufficient background[17, 20]. It has recently been shown that shelterin components, TRF1, Pot1b, and Tpp1, critically regulate HSC activity and survival[21-23]. However, due to embryonic lethality, the role of Pot1a in maintaining HSC function is still unclear and it is not known if POT1/Pot1a has a non-telomeric role in HSC regulation and maintenance.

Here, we show that Pot1a maintains HSC activity by protecting against DNA damage and preventing the production of reactive oxygen spices (ROS). Due to these protective functions, we find that treatment with exogenous Pot1a maintains HSC self-renewal and function *ex vivo* and improves the activity of aged HSCs.

Results

Pot1a expression in HSCs

First, we analyzed the expression of Pot1a in haematopoietic stem, progenitor and differentiated cells. We observed that Pot1a is expressed at substantially higher levels in short-term (ST)- and long-term (LT)-HSC fractions than in progenitor and differentiated cell fractions (Fig. 1a-d), yet this expression sharply decreases with age (Fig. 1e-g). Other components of the shelterin complex were also more highly expressed in HSC fractions than in progenitor and differentiated cell fractions (Supplementary Fig. 1a) and showed similar expression changes with aging, with the exception of Terf1 and Rap1 (Supplementary Fig. 1b). These data indicate a close correspondence between Pot1a expression and aging in LT-HSCs.

Loss of Pot1a compromises LT-HSC activity

To investigate the function of Pot1a in the regulation of HSC maintenance, we transduced retrovirus-expressing Pot1a-specific shRNAs (shPot1a-1 and -2) into lineage$^-$Sca-1$^+$c-Kit$^+$ (LSK) CD41$^-$CD48$^-$CD150$^+$ cells. Both Pot1a shRNAs substantially suppressed Pot1a expression at both the mRNA and protein levels (Supplementary Fig. 2a, b). We then analyzed the effect of Pot1a knockdown on the function of HSCs. Knockdown of Pot1a decreased both the number of colony forming units in culture (CFU-Cs) and high proliferative potential colony forming cells (HPP-CFCs) (Supplementary Fig. 2c, d). Furthermore, while transduction of shPot1a increased total cell numbers it also inhibited LT-HSC proliferation and induced apoptosis of LT-HSCs in culture (Supplementary Fig. 2e-g), suggesting that loss of *Pot1a* compromises HSC activity *in vitro*. Knockdown of Pot1a also markedly reduced donor cell engraftment after BM transplantation (BMT) in peripheral blood (PB), LSK and LT-HSC fractions (Supplementary Fig. 2h, j), and induced a bias toward myeloid and away from lymphoid differentiation (Supplementary Fig. 2i). Similar results have been previously observed with *Tpp1* deficiency[21]. Since TPP1 is required for the binding of POT1 to telomeres[24], this suggests that the function of Pot1a at telomeres is critical for HSC maintenance. To confirm the specificity of these results we co-transduced shPot1a and a silent mutant Pot1a (smPot1a), which has silent mutations within the shRNA targeting sequences, into LT-HSCs and transplanted them into lethally irradiated recipient mice. Expression of Pot1a was restored in co-transduced cells, and they accordingly showed substantially better engraftment than those that were transduced with shPot1a-1 or -2 alone (Supplementary Fig. 2k), indicating that expression of smPot1a was able to rescue the BM reconstitution activity of Pot1a knockdown HSCs.

To investigate these results further we then analyzed the effect of Pot1a knockdown on HSC gene expression patterns. First, we checked the expression levels of other shelterin components after Pot1a knockdown and found that the knockdown of Pot1a decreased the expression of *Pot1b* and *Tpp1* but did not affect the expression levels of other shelterin

components (Supplementary Fig. 3a). We then examined the expression of genes related to HSC aging, maintenance, apoptosis, and differentiation. Analysis of gene expression patterns revealed that Pot1a knockdown upregulated expression of genes associated with senescence/apoptosis and differentiation, and downregulated expression of genes required for HSC maintenance (Supplementary Fig. 3b). Collectively, these data suggest that Pot1a has an important role in regulating the proliferation, differentiation, and maintenance of LT-HSCs both *in vitro* and *in vivo*.

Overexpression of Pot1a enhances HSC function

To dissect Pot1a function further, we transduced a retrovirus-expressing Pot1a into LSK cells to assess the effect of Pot1a overexpression on stem cell function. We first checked whether Pot1a overexpression affects the level of other shelterin components and we found that the transduction of Pot1a did not change the expression level of other shelterin genes (Supplementary Fig. 4a). Next, we checked the effect of Pot1a overexpression on the function of LT-HSCs. As expected, overexpression of Pot1a substantially increased the numbers of CFU-Cs and HPP-CFCs, and colony sizes in culture (Fig. 2a-e). In accordance with this enhanced colony forming ability, expression of HSC markers was also upregulated (Supplementary Fig. 4b). To assess whether overexpression of Pot1a in culture affects self-renewal of HSCs *in vivo*, LSK cells overexpressing Pot1a were cultured for 7 or 14 days and then transplanted into lethally irradiated mice. Overexpression of Pot1a was observed to facilitate donor cell engraftment (Fig. 2f), indicating that in addition to maintaining HSC numbers, exogenous Pot1a also preserves the long-term reconstitution (LTR) ability of HSCs during *in vitro* culture. To investigate further, we examined the effect of Pot1a overexpression on maintenance of HSC self-renewal activity in serial BMT. Pot1a overexpression had no effect on donor cell engraftment in PB in primary BMT, although it did increase the proportion of donor-derived

ST- and LT-HSC fraction compared with control GFP-transduced cells (Fig. 3a, Supplementary Fig. 5a and b). Upon secondary BMT we found that Pot1a overexpression substantially increased reconstitution in the PB, BM LSK, and LT-HSC fractions (Fig. 3c). Furthermore, Pot1a overexpression maintained a $Ki67^{-}$ quiescent population in the donor-derived LSK fraction after primary and secondary BMT (Supplementary Fig. 5c). Notably, in contrast to Pot1a knockdown, Pot1a overexpression induced a distinct bias towards lymphoid differentiation and away from myeloid differentiation in donor cells (Fig. 3b, d). Taken together these data indicate that overexpression of Pot1a enhances the functional activity of HSCs *in vivo*.

Pot1a regulates HSC self-renewal by preventing DDR

To determine the mechanisms by which Pot1a regulates HSC activity we sought to assess the role of Pot1a in the protection of DDR signaling. Telomere dysfunction-induced foci (TIFs), a marker for DNA damage at telomeric DNA[25], were identified by co-localization of 53BP1 and TRF1. Significant co-localization of 53BP1 and TRF1 was determined by image analysis (see Methods and Supplementary Table 1). We first observed that Pot1a knockdown increased the number of TIFs in LSK cells in culture (Fig. 4a, b). In order to determine whether the formation of TIFs in LT-HSCs was due to ATR signaling, we then measured the expression of replication protein A 32 kDa subunit (RPA32, a ssDNA binding protein that activates the ATR kinase pathway[8]) and phosphorylated Chk1 (pChk1, which has a critical role in DNA damage checkpoint control and tumor suppression[26, 27]) by immunocytochemistry, following BMT of control GFP or Pot1a overexpressing HSCs. We observed that HSCs overexpressing Pot1a had significantly fewer TIFs than controls 4 months after BMT (Fig. 4c, d) and expression of RPA32 (Fig. 4e) and phosphorylated Chk1 (Fig. 4f) were reduced upon Pot1a overexpression. Furthermore, Pot1a overexpression substantially reduced the phosphorylation of Chk1 after a

second BMT (Fig. 4g). Interestingly, in addition to TIFs, we also observed that the total number of 53BP1 foci and the overall level of 53BP1 expression in LT-HSCs was increased by Pot1a knockdown and was decreased by Pot1a overexpression (Supplementary Fig. 6), suggesting that Pot1a protects both telomeric and extra-telomeric DNA in HSCs. We also found that overexpression of Pot1a increased telomerase activity in HSCs (Supplementary Fig. 4c), while Pot1a overexpression did not alter telomere length in donor-derived cells isolated 4 months after primary BMT (Supplementary Fig. 4d, e). These results indicate that the protection of both telomeric and non-telomeric DDR by Pot1a is important for the maintenance of HSC function.

Pot1a prevents the production of ROS in LT-HSCs

Since we observed that Pot1a expression is negatively associated with 53BP1 levels, we sought to clarify how Pot1a regulates non-telomeric DDR in LT-HSCs. To do so, we performed microarray analysis of control-GFP and Pot1a-transduced LT-HSCs (Fig. 5a). Gene set enrichment analysis (GSEA) revealed that Pot1a transduction reduced the expression of genes associated with oxidative phosphorylation, mitochondrial respiratory chain, and oxygen and reactive oxygen species metabolic processes by comparison with controls (Fig. 5b). Since oxidative stress induced by ROS is known to induce DNA damage[6] and reduce the self-renewal activity of HSCs[28], these data suggested that Pot1a might be preventing the production of ROS in HSCs in culture. To test this further, we assessed the relationship between Pot1a expression and ROS production in LT-HSCs (Fig. 5c) and found that overexpression of Pot1a substantially reduced overall levels of intracellular ROS as well as mitochondrial ROS by comparison with controls (Fig. 5d-f). Since activation of the mTOR pathway leads to ROS production[29, 30] we also examined the expression of mTOR (*Mtor*) and Raptor (*Rptor*) mRNA in Pot1a overexpressing or knockdown LT-HSCs (Fig. 5g-i). We found that overexpression of Pot1a substantially decreased *Mtor* and *Rptor* expression (Fig. 5h), while knockdown of Pot1a

184 substantially increased *Mtor* and *Rptor* expression (Fig. 5i). Although the mechanistic details
185 are not currently clear, these data suggest that Pot1a plays a part in preventing the activation of
186 mTOR signaling and production of ROS that may contribute to the maintenance of LH-HSCs.
187
188 **POT1a protein inhibits DDR and maintains HSC in culture**
189 Since Pot1a overexpression is able to maintain HSC activity, we next sought to
190 determine if treatment with exogenous POT1a protein has a similar effect. For this purpose, we
191 prepared a recombinant mouse POT1a protein (MTM-POT1a) with 6xHis and membrane-
192 translocating motif (MTM)-tags (Supplementary Fig. 7a) to facilitate cellular uptake[31, 32]. This
193 method allows Pot1a protein to be delivered without retroviral transduction and therefore does
194 not risk insertional mutagenesis. HSCs incorporated MTM-POT1a at high efficiency (>90%)
195 within 2 hours, and the incorporated protein was detectable in LSK cells at least 96 hours after
196 culture (Supplementary Fig. 7b, c). Co-staining of Pot1a with TRF1 confirmed that MTM-
197 POT1a was appropriately localized to telomere regions (Supplementary Fig. 7d). Culture of LT-
198 HSCs with MTM-POT1a enhanced CFU-C and HPP-CFC numbers (Fig. 6a). Furthermore,
199 MTM-POT1a increased the numbers of LT-HSCs in culture (Fig. 6b). Interestingly, treatment
200 with MTM-POT1a did not affect cellular survival rate in culture (Fig. 6c) but was able to inhibit
201 Pot1a knockdown-induced apoptosis of LT-HSCs (Fig. 6d). These data suggest that Pot1a
202 prevents differentiation of LT-HSCs in culture. Similarly, in cases when Pot1a expression has
203 been lost (e.g. due to ageing) exogenous Pot1a improves HSC survival. As was the case with
204 Pot1a overexpression, treatment with MTM-POT1a inhibited DDR in LT-HSCs after 3 weeks of
205 culture (Fig. 6e) and treatment with MTM-POT1a substantially increased LT-HSC numbers in
206 culture over the same time period (Fig. 6f). However, cell cycle analysis, using LT-HSCs
207 derived from the Fucci mouse[33], showed that MTM-POT1a did not affect the frequencies of
208 S/G2/M cells in HSPCs in culture (Supplementary Fig. 7e, f). Taken together these results

indicate that Pot1a maintains LT-HSC fraction in culture by preventing DNA damage rather than affecting the rate of cell division directly.

Recombinant POT1a maintains self-renewal activity of LT-HSCs

We next examined the effect of exogenous POT1a protein on HSC function and sought to assess the extent to which treatment with MTM-POT1a was able to preserve stem cell function *ex vivo* by performing serial BMTs of control MTM protein and MTM-POT1a treated LT-HSCs. We observed that culture with MTM-POT1a for 10 days prior to transplantation substantially increased the chimerism of donor-derived cells after the first transplantation by comparison with controls (Fig. 7a). PB analysis showed that treatment with MTM-POT1a did not affect the ability of donor-derived cells to differentiate into myeloid, B cells, and T cell lineages (Fig. 7b), indicating maintenance of robust multi-lineage reconstitution. In addition, BM cells isolated from recipient mice transplanted with MTM-POT1a treated cells again showed substantially increased chimerism and robust multi-lineage reconstitution (Fig. 7c, d). Importantly, mutant forms of the MTM-POT1a proteins that lack the OB-fold domains (MTM-POT1aΔOB) or TPP1-binding domain (TBD) (MTM-POT1aΔTBD) (Supplementary Fig. 8a, b) did not prevent telomeric DDR in LT-HSCs in culture (Supplementary Fig. 8c, d). Additionally, these deletion mutant POT1a proteins did not affect long-term engraftment of HSCs (Fig. 7e), HSC colony forming ability in culture (Supplementary Fig. 8e), telomerase activity in culture (Supplementary Fig. 8f), or LT-HSC numbers *in vitro* (Supplementary Fig. 8g). To clarify the long-term effect of the overexpression of mutant forms of Pot1a, we transplanted Pot1aΔOB and Pot1aΔTBD transduced LT-HSCs. In contrast to treatment with MTM protein, overexpression of mutant forms of Pot1a inhibited the long-term engraftment of donor HSCs (Fig. 7f). These results indicate that the binding of Pot1a to telomeric DNA as part of the shelterin complex is critical for the maintenance of HSC function.

To further verify these results we also conducted limiting dilution competitive BMT. We observed that populations treated with MTM-POT1a had a 3-fold enrichment for functional LT-HSCs in comparison with populations treated with control MTM protein (Fig. 7g). Taken together these data suggest that treatment with exogenous Pot1a enhances the self-renewal activity of HSCs in culture.

Exogenous POT1a improves the activity of aged LT-HSCs

To investigate the activity of Pot1a during aging we next analyzed the effect of MTM-POT1a on the prevention of TIF formation in aged LT-HSCs. As expected we found that aged (>90 week-old) LT-HSC had more TIFs than young (8 week-old) LT-HSCs, yet importantly treatment with MTM-POT1a reduced the number of TIFs in cells isolated from both young and old mice after 10 days of culture (Supplementary Fig. 9). We also examined the effect of MTM-POT1a treatment on the proliferation and apoptosis of aged LT-HSCs. In accordance with the effect that we observed in young LT-HSCs (Fig. 6b, c), treatment of MTM-POT1a increased aged LT-HSC numbers in culture without affecting the total cell number and apoptosis compared with control MTM protein treatment (Fig. 8a-c).

To determine the potency of these effects we sought to assess if treatment with Pot1a was able to restore the activity of aged HSCs in culture. To do this, we compared the reconstitution activity following BMT of LT-HSCs isolated from young (8 week-old) and aged (>90 week-old) after culture with MTM-POT1a or control MTM protein. As expected, after 10 days of culture the reconstitution activity of aged HSCs was substantially lower than that of young HSCs (Fig. 8d). However, MTM-POT1a treatment raised the engraftment ability of aged HSCs compared with control MTM treatment (Fig. 8d). In addition, aged controls showed a decrease in B cell and an increase in myeloid cell differentiation, while treatment with MTM-POT1a diminished this bias (Fig. 8e).

To further understand the function of exogenous Pot1a in the activation of aged HSCs, we performed microarray analysis of control and MTM-POT1a treated aged HSCs. GSEA revealed that aged HSCs cultured with control MTM protein had a tendency to express myeloid-associated genes in culture, while MTM-POT1a treated aged HSCs did not (Fig. 8f). Conversely, MTM-POT1a treated HSCs significantly overexpressed genes associated with long-term HSC identity (Fig. 8f). These results suggest that MTM-POT1a treatment inhibits myeloid differentiation and helps maintain the undifferentiated LT-HSC state.

In addition, similar to our observations in 8 week-old LT-HSCs, we found that genes associated with oxidative phosphorylation, the mitochondrial respiratory chain, Myc targets, E2F targets, DNA repair and DNA replication were suppressed in aged HSCs cultured with MTM-POT1a by comparison with control MTM treated aged HSCs (Supplementary Fig. 10a). Furthermore, as with young LT-HSCs, overexpression of Pot1a significantly decreased *Mtor* and *Rptor* expression (Supplementary Fig. 10b) and reduced the production of ROS in aged LT-HSCs during culture (Supplementary Fig. 10c-e).

POT1 expands human LT-HSC numbers

Based on the functional effect of MTM-POT1a on mouse HSCs, we sought to determine whether exogenous human POT1 similarly affects human HSC activity. We observed that human cord blood (hCB)-derived $Lin^-CD34^+CD38^-CD90^+CD45RA^-CD49f^+$ LT-HSCs [34] expressed significantly higher levels of *POT1* than $CD34^+$ HSPCs (Fig. 9a). To assess the effect of POT1 on human HSC activity we prepared MTM-POT1 recombinant protein (Supplementary Fig. 7a) and cultured human CB and BM LT-HSCs with MTM-POT1 for 10 days. In accordance with the role of MTM-POT1a in mouse, MTM-POT1 significantly increased the number of CFU-Cs and HPP-CFCs from hCB LT-HSCs (Fig. 9b) and markedly reduced total and telomeric DDR (Fig. 9c, d). Although it did not affect the total cell number or number of

284 $CD34^+CD38^-$ cells, treatment with MTM-POT1 significantly increased the number of LT-HSCs
285 in culture of CB-derived HSCs (Fig. 10a, b) but did not influence LT-HSC apoptosis (Fig. 10c).
286 Similarly, the treatment of BM-derived LT-HSCs with MTM-POT1 also increased the number
287 of $Lin^-CD34^+CD38^-$ cells and $Lin^-CD34^+CD38^-CD90^+CD45RA^-CD49f^+$ LT-HSCs in cultures
288 (Fig. 10d). In accordance with these results we observed that populations treated with MTM-
289 POT1 contained 4.5-fold more functional LT-HSCs in comparison with controls following
290 limiting dilution BMT (Fig. 10e). Collectively, these data indicate that POT1 regulates human
291 HSC activity in a similar manner to that of Pot1a in mice, and may be used to efficiently
292 maintain human HSC activity *ex vivo*.
293
294 **Discussion**
295 Taken together our data demonstrate that Pot1a has a critical role in maintaining HSC
296 activity during long-term *in vitro* culture or subsequent to BMT. We found that Pot1a regulates
297 HSC activity by inhibiting ATR-dependent telomeric DNA damage, and thereby protecting cells
298 from associated apoptosis. These results indicate that the formation of the shelterin complex at
299 the telomeric region is important to Pot1a mediated maintenance of LT-HSC activity. However,
300 in addition to this telomeric role we have also identified a novel non-telomeric role. This new
301 non-telomeric role is particularly interesting since reduction of ROS is thought to be crucial in
302 inhibiting global DNA damage in LT-HSCs in culture. Energy metabolism in quiescent HSCs
303 largely depends on glycolysis, while activated HSCs synthesize adenosine-5'-triphosphate
304 (ATP) mainly through oxidative phosphorylation[35, 36]. Our finding that HSCs upregulate genes
305 associated oxidative phosphorylation in culture suggests that culture induces a metabolic shift
306 from glycolysis to oxidative phosphorylation that is characteristic of stress-induced activation,
307 yet this shift can be inhibited by Pot1a treatment. Moreover, we observed that Pot1a expression
308 is negatively associated with mTOR expression in HSCs. This suggests that Pot1 may have an

important role in regulating mTOR signaling, although further work to dissect the details of this non-telomeric role for Pot1a in the maintenance of HSC activity is needed.

In addition to its role in protecting against stress we also found that Pot1a has a central role in regulating stem cell activity during aging. We observed that expression of Pot1a is lost during aging, and this loss results in the accumulation of DNA damage, alterations in metabolism and an increase in ROS production, which in turn compromises aged HSC function. However, we observed that this decline is reversible: remarkably *ex vivo* treatment of aged LT-HSCs with recombinant POT1a is able to re-activate aged HSCs. Since Pot1a overexpression inhibited the expression of *Mtor* and *Rptor* in aged LT-HSCs, the regulation of mTOR signaling by Pot1a may participate in this re-activation of aged HSC function. Although the precise mechanisms by which this functional improvement occurs have yet to be fully determined, our results indicate that exogenous Pot1a can both prevent telomeric and non-telomeric DNA damage and inhibit ROS production, thereby inducing a more potent immature phenotype in aged HSCs upon *ex vivo* culture. It will be interesting to clarify how these mechanisms are related to one another and determine, for example, whether telomere insufficiencies precede metabolic changes and ROS production or vice versa.

Since a similar protective role for POT1 was also seen in human HSCs these results have important implications for the culture of human HSCs *ex vivo*. Expansion of HSC numbers requires the stimulation of self-renewal divisions[37]. Although a number of strategies, including culture with recombinant proteins[38-41], modulation of intrinsic factors, such as Hoxb4[42-44], Prostaglandin E2[45], or aryl hydrocarbon receptor antagonist[46, 47] have been reported to contribute to HSC expansion in culture, these treatments primarily work by activating the cell cycle. By contrast, we find that Pot1a does not directly activate the cell cycle of HSCs, but rather protects HSCs from DNA damage under stress. Based on these findings, we anticipate that, in

combination with current methods, POT1 will be of significant use in the development of robust and safe methods for *ex vivo* expansion of human HSCs.

Taken together our results highlight general telomeric and non-telomeric mechanisms by which Pot1 regulates stem cell activity *in vitro* and *in vivo*, with widespread implications for our understanding of age-related degeneration and applications in regenerative medicine.

Methods

Mice and cells

C57BL/6 (B6-Ly5.2), C57BL/6 mice congenic for the Ly5 locus (B6-Ly5.1) were purchased from Sankyo-Lab Service (Tsukuba, Japan). Fucci mice were provided by Dr. Miyawaki (Brain Science Institute, RIKEN, Wako-city, Saitama, Japan). Tert mutant mice were provided by Dr. Ishikawa (Kyoto University, Kyoto, Japan). Female NOD/SCID/IL-2Rc^{null} (NOG) mice were purchased from the Central Institute for Experimental Animals (Chiba, Japan) and bred in a pathogen-free environment. In this study, female mice were used for all experiments except the microarray analysis. hCB-derived CD34^{+} cells (catalog number: 2C-101B) and hBM-derived CD34^{+} cells (catalog number: 2M-101) were purchased from Lonza. The Gene recombination experiment safety committee and animal experiment committee in both Keio University and Kyushu University approved this study and all experiments were carried out in accordance with the Guidelines for Animal and Recombinant DNA experiments at Keio University and Kyushu University.

Mouse antibodies

The following monoclonal antibodies (Abs) were used for flow cytometry and cell sorting: anti-c-Kit (2B8, BD Biosciences, 1:100), -Sca-1 (E13-161.7, BD Biosciences, 1:100), -CD3e (145-2C11, BD Biosciences, 1:100), -CD4 (RM4-5, BD Biosciences, 1:100), -CD8 (53-6.7, BD

Biosciences, 1:100), -B220 (RA3-6B2, BD Biosciences, 1:100), -TER-119 (BD Biosciences, 1:100), -Gr-1 (RB6-8C5, BD Biosciences, 1:100), -Mac-1 (M1/70, BD Biosciences, 1:100), -Flt3 (A2F10.1, BD Biosciences, 1:100), -CD41 (MWReg30, eBioscience, 1:100), -CD48 (HM48-1, Biolegend, 1:100), -CD150 (TC15-12F12.2, Biolegend, 1:100), -CD45.1 (A20, BD Biosciences, 1:100), -CD45.2 (104, BD Biosciences, 1:100), -CD45 (30-F11, BD Biosciences, 1:100), and -Ki67 (B56, BD Biosciences, 1:30). A mixture of CD4, CD8, B220, TER-119, Mac-1, and Gr-1 was used as the lineage mix. Anti-Chk1 (sc-8408, Santa Cruz Biotechnology, 1:100), anti-Phospho Chk1 (133D3, Cell Signaling Technology, 1:100), and anti-53BP1 (NB100-304, Novus biologicals, 1:100) were used for the analysis of the phosphorylation of Chk1 and 53BP1 by FACS. The following Abs were used for immunocytochemistry and immunoblotting: anti-POT1 (ab21382, Abcam for immunocytochemistry, 1:200. sc-27951, Santa Cruz Biotechnology for immunoblotting, 1:1000), anti-53BP1 (NB100-304, 1:200), anti-TRF1 (sc-5475, Santa Cruz Biotechnology, 1:200), anti-RPA32 (sc-28709, Santa Cruz Biotechnology, 1:200), anti-phospho Chk1 (ab47318, Abcam, 1:200), and anti-His-Tag (ab27025, Abcam, 1:200).

Human antibodies

The following monoclonal Abs were used for flow cytometry and cell sorting: anti-CD34 (581, BD Biosciences, 1:5), -CD38 (HIT2, BD Biosciences, 1:5), -CD45RA (HI100, BD Biosciences, 1:20), -CD90 (5E10, BD Biosciences, 1:20), -CD49f (GoH3, Biolegend, 1:5), and -CD45 (HI30, BD Biosciences, 1:20). A mixture of biotin-conjugated anti-CD2, -CD3, -CD11b, -CD14, -CD15, -CD16, -CD19, -CD56, -CD123, and -CD235a (130-092-211, Lineage Cell Depletion Kit human, Miltenyi Biotec Inc., 1:5) was used as the lineage mix. The following Abs were used for immunocytochemistry: anti-human TRF1 (TRF-78, ab10579, Abcam, 1:100), 53BP1 (NB100-304, 1:200), and RPA32 (sc-28709, 1:200).

Cell preparation and flow cytometry

BM cells were isolated from femurs and tibias by flushing with PBS. Mononuclear cells (MNCs) were isolated by centrifugation of total BM cells on Lymphoprep™ (Alere Technologies AS). For isolation of mouse HSCs, c-Kit$^+$ cells were enriched by magnetic cell sorting with anti-CD117 beads (130-091-224, Miltenyi Biotec Inc. 1:5 dilution). c-Kit enriched cells were stained with lineage marker Abs (anti-CD4, -CD8, -B220, -Gr1, -Mac-1, -Ter119, anti-Sca-1, anti-c-Kit, anti-CD48, and anti-CD150). For isolation of human HSCs, hCB and hBM CD34$^+$ cells were stained with a mixture of biotin-conjugated lineage Abs (anti-CD34, -CD38, -CD45RA, -CD90, -CD49f) and a fluorochrome labeled streptavidin (1:100 dilution). Stained cells were analyzed and sorted using a FACSAria (BD Biosciences).

Immunocytochemistry

Cells were spread onto glass slides and fixed in 4% paraformaldehyde/PBS(−) or methanol/acetone. After blocking, samples were incubated at 4°C overnight with a primary Ab. After washing with PBS, samples were stained with florescence-labeled secondary Ab. For nuclear staining, specimens were treated with TOTO3 or DAPI (Molecular Probes, 1:300). Fluorescence images were examined using a confocal laser-scanning microscope (FV1000, Olympus or LSM700, Zeiss).

Image analysis

Assessment of co-localization of staining for TRF1 (green) and 53BP1 or RPA32 (red) was conducted as previously described[48, 49]. Briefly, subsequent to thresholding using Otsu's method[50], the extent of co-localization for each image was determined using Manders' co-localization coefficients

$$\mathrm{M1} = \frac{\sum_i G_{i,\,\mathrm{colocal}}}{\sum_i G_i}$$

$$\mathrm{M2} = \frac{\sum_i R_{i,\,\mathrm{colocal}}}{\sum_i R_i}$$

where R_i and G_i are the intensities of the *i*th pixel in the red and green channels respectively, and $R_{i,\,\mathrm{colocal}} = R_i$ if $G_i > 0$ and zero otherwise (and similarly for $G_{i,\,\mathrm{colocal}}$). Significance of co-localization was obtained by comparing observed co-localization coefficients with those obtained by independently scrambling the red and green channels 1×10^4 times. Note that since the number of red and green pixels may differ, M1 and M2 are not generally equal. Random scrambling of pixels does not preserve local spatial correlations in pixel intensities and can lead to overestimation of the significance of colocalization[48]. Therefore, the binary images from both channels were randomly divided into blocks approximately the size of a TIF and these blocks (rather than individual pixels) were scrambled, as previously described[48]. This method preserves local spatial correlations in pixel intensities and therefore provides a conservative null model. Significance of co-localization was determined by calculating the proportion of times that randomization increased the overlap coefficients M1 and M2 relative to the coefficients obtained prior to scrambling and by comparing observed and randomized co-localization coefficients using Welch's paired t-test. All analysis was restricted to regions identified as cell nuclei using co-staining for TOTO3 (blue). In total co-localization in >3750 cells from >1000 independent images were assessed.

Immunoblot analysis

To evaluate Pot1 expression levels in hematopoietic stem/progenitor cells, BM Lin^+, Lin^-, $LSK150^-$, and $LSKCD150^+$ cells (1×10^5 cells) were lysed and subjected to SDS-PAGE and immunoblotting using antibodies against POT1 polyclonal Ab (Santa Cruz Biotechnology, Inc.) (1:1000). Rabbit anti-Goat IgG HRP (DAKO) (1:5000) was used for the secondary Ab.

Densitometric quantification was performed on scanned immunoblot images using Multi Gauge V3.1 (Fuji Film). To evaluate the efficiency of Pot1a knockdown, LT-HSCs were transduced with retrovirus expressing control-sRNA, shPot1a-1 or -2. After 2 days of the transduction of shRNA, GFP^+ $LSKCD150^+$ (1×10^5 cells) were isolated and analyzed Pot1 expression by western blot. All uncropped western blots can be found in Supplementary Fig. 11.

Q-PCR analyses

Q-PCR analysis was performed on an ABI 7500 Fast Real-Time PCR System using TaqMan Fast Universal PCR master mixture (Applied Biosystems, Foster City, CA, USA). The TaqMan® Gene Expression Assay mixes used in this study are listed below. Data were analyzed by 7500 Fast System SDS Software 1.3.1. All experiments were carried out in triplicate.

Q-PCR array analysis

Gene expression was analyzed using the BioMark 96·96 Dynamic Array (Fluidigm). Data were analyzed using BioMark Real-Time PCR Analysis Software Version 3.0.2 (Fluidigm). The TaqMan Gene Expression Assay Mixes used in this study are listed below**.**

TaqMan® Gene Expression Assay Mixes

TaqMan® Gene Expression Assays used in this study are listed in Supplementary Tables 2 and 3.

Intracellular flow cytometry

For the staining of intracellular antigen, cells were first stained with cell surface markers prior to fixation and permeabilization. Cells were then fixed and permeabilized with Cytofix/Cytoperm™ (BD Bioscience) and stained with Abs against the intracellular antigen.

Apoptosis was analyzed by Annexin V assay Kit (BioLegend). ROS level was measured using CellROX® Reagents (Thermo Fisher Scientific) and MitoSOX™ Red (Thermo Fisher Scientific).

Quantification of telomere length and telomere FISH

Telomere length was quantified by flow cytometry using flow FISH with a Telomere PNA Kit/FITC for flow cytometry (Dako Cytomation), according to the manufacturer's instructions. In brief, Pot1a or control-mKO1 transduced LSK cells were divided into 2 tubes, denatured in hybridization solution with or without telomere-PNA probes, and hybridized overnight. After washing and DNA staining, the labeled or non-labeled (control) samples were analyzed by FACS.

Quantitative telomeric repeat amplification protocol

Telomerase activity was measured with a Q-TRAP assay and used a Quantitative Telomerase Detection Kit (US Biomax, Inc.). In this assay, sorted cells were lysed, and the lysate was added to telomeric repeats onto a substrate oligonucleotide. The resultant extended product was subsequently amplified by PCR. Direct detection of PCR product was monitored on an ABI 7500 Fast Real-Time PCR System.

Sequences of Pot1a shRNAs

The sequences of Pot1a shRNAs were as follows: shPot1a-1, 5′-GGAAGGTACAATTGCCAAT-3′; shPot1a-2, 5′-GCCTCCGTATGTTAGCAAA-3′. Sequences were separated by a nine-nucleotide non-complementary spacer (TTCAAGAGA) from the corresponding reverse complement of the same 19-nucleotide sequence. A scrambled sequence (5′-GACACGCGACTTGTTGTACCAC-3′) served as a control.

Construction of retroviral vectors

For the construction of the retrovirus vector-expressing mouse Pot1a, full-length cDNA of mouse Pot1a (OriGene Technologies, Inc.) was ligated into pMY-IRES-GFP (provided by Dr. Kitamura; University of Tokyo, Institute of Medical Science) or pMY-IRES-monomeric Kusabira-Orange1 (mKO1). For construction of Pot1a-shRNA retroviral vectors, oligonucleotides were inserted into pRetroU6-PGK/EGFP (gift from Dr. Takahiko Hara, The Tokyo Metropolitan Institute of Medical Science) at the BglII and HindIII sites and cloned as a retroviral vector.

Retroviral transduction

Freshly isolated LSK, LSKFlt3$^-$ cells or LSKCD41$^-$CD48$^-$CD150$^+$ cells were pre-cultured for 1 day in SF-O3 medium (EIDIA Co., Ltd.) in the presence of 0.1% BSA, 100 ng ml^{-1} stem cell factor (SCF) (PeproTech), and 100 ng ml^{-1} thrombopoietin (TPO) (PeproTech), and then transfected with retrovirus-expressing Pot1a or shPot1a on RetroNectin™ (Takara Bio Inc.) using Magnetofection^{TM} (OZ Biosciences) according to the manufacturer's instructions. The cells were then cultured for one day at 37°C in 5% CO_2. The efficiency of Pot1a overexpression or suppression in HSCs was confirmed by Q-PCR.

Microarray analysis

Aged LT-HSCs (60 week-old) were cultured in SF-O3 medium in the presence of BSA (0.1%), SCF (100 ng ml^{-1}), and TPO (100 ng ml^{-1}) with control or MTM-POT1a protein for 3 days. After culture total RNA was isolated from cells using RNeasy Mini Kit (Qiagen) according to the manufacturer's instructions. RNA samples were quantified by an ND-1000 spectrophotometer (NanoDrop Technologies, Wilmington, DE) and the quality was confirmed

with a 2200 TapeStation (Agilent technologies, Santa Clara, CA). The cRNA was amplified, labeled with 10 ng of total RNA using GeneChip® WT Pico Kit and hybridized to a Affymetrix GeneChip® Mouse Gene 2.0 ST Array array according to the manufacturer's instructions. All hybridized microarrays were scanned by an Affymetrix scanner. Relative hybridization intensities and background hybridization values were calculated using Affymetrix Expression Console™. Raw signal intensities for each probe were calculated from hybridization intensities. Raw signal intensities were log2-transformed and normalized by RMA and quantile algorithms[51] with Affymetrix® Expression Console™ 1.1 software. Gene set enrichment analysis (www.broadinstitute.org/gsea) was performed to determine whether the predefined gene sets were enriched in control or MTM-POT1a treated aged HSCs. The microarray data have been deposited in the Gene expression omnibus (GEO, http://www.ncbi.nlm.nih.gov/geo/) database, and have been assigned accession numbers GSE86386 and GSE85016.

Production of MTM proteins

The plasmid pET28a-MTM/N1-POT1a or POT1 was constructed by cloning full-length Pot1a or POT1 cDNA into the pET28a-MTM N1 vector (Supplementary Fig. 7). His-MTM-POT1a and POT1 were expressed in *E. coli* BL21 (DE3) cells transformed with pET28a-MTM/N1-POT1a or pET28a-MTM/N1-POT1 plasmids. Cells were grown at 37°C in LB medium supplemented with kanamycin (100 μg ml^{-1}) to reach an optical density (OD600 nm ~0.6). To induce the expression of the recombinant protein, 0.1mM isopropyl thiogalactoside was added to the culture medium and the cells cultured for an additional 3 hours at 37°C. After culture, the cells were harvested. Recombinant protein was purified using a Ni-NTA purification system (Life Technologies Corporation), according to the manufacturer's instructions. The His-MTM peptide was used as the control. Mutant forms of Pot1a were constructed by cloning Pot1aΔOB

529 or Pot1aΔTBD cDNA into the pET28a-MTM N1 vector. MTM-POT1aΔOB and MTM-
530 POT1aΔTBD were purified by same procedure as described above.
531
532 **Long-term culture and colony formation assay**
533 To analyze the effect of the overexpression or knockdown of Pot1a on colony-forming activity,
534 Pot1a- or shPot1a-transduced LSK cells were cultured for 1-4 weeks. After *in vitro* culture,
535 GFP^+ LSK cells were sorted and cultured in MethoCult™ GF M3434 medium for mouse cells
536 and MethoCult™ H4034 for human cells (Stemcell Technologies).
537 To analyze the effect of MTM-POT1a on the maintenance of HSC colony formation activity,
538 $LSKCD41^-CD48^-CD150^+$ cells were cultured for 10 days in SF-O3 medium in the presence of
539 0.1% BSA, 100 ng ml^{-1} SCF, and 100 ng ml^{-1} TPO with or without MTM-POT1a. Lin^- cells
540 were sorted and their ability to form colonies was then assessed. To analyze the effect of MTM-
541 POT1a on the maintenance of HSC numbers, LT-HSCs ($LSKCD41^-CD48^-CD150^+$ cells) were
542 cultured for 3 weeks in SF-O3 medium in the presence of 0.1% BSA, 100 ng ml^{-1} SCF, and 100
543 ng ml^{-1} TPO with or without MTM-POT1a. After culture, the number of LSK cells and LT-
544 HSCs was examined. For examination of colony formation in hCB HSCs after *in vitro* culture,
545 $Lin^-CD34^+CD38^-CD45RA^-CD90^+CD49f^+$ cells were cultured for 10 days in StemSpan SFEM
546 (Stemcell Technologies) in the presence of 100 ng ml^{-1} SCF, 100 ng ml^{-1} rhFL, and 20 ng ml^{-1}
547 TPO with or without MTM-POT1. After culture, Lin^- cells were sorted and cultured in
548 MethoCult™ H4034 medium.
549
550 ***In vitro* culture and immunostaining**
551 To analyze the effect of MTM proteins (control, Pot1a, Pot1aΔOB, and Pot1aΔTBD) on the
552 inhibition of DDR in HSCs, $LSKCD41^-CD48^-CD150^+$ cells were cultured for 10 days. LT-
553 HSCs were then re-sorted from cultures and stained with either anti-TRF1 as a marker of the

telomeric DNA region, anti-53BP1 as a marker of DNA damage, or anti-RPA32 and -phosphor-Chk1 for ATR signaling.

BMT assay of Pot1a-overexpressed and knockdown HSCs

To evaluate the function of Pot1a in the regulation of LTR activity, $Ly5.1^+$ LSK cells (8 week-old) were transduced with retroviruses expressing Pot1a or Pot1a shRNAs. After retroviral transduction, GFP^+LSK cells (5×10^3 cells $mice^{-1}$) were transplanted into lethally irradiated $Ly5.2^+$ mice using 2×10^5 competitor cells (first BMT). The percentage of donor-derived GFP^+ cells in PB was analyzed monthly by flow cytometry. Sixteen weeks after the first BMT, the percentages of donor-derived ($GFP^+Ly5.1^+$) cells in the BM LSK and $LSKCD41^-CD48^-CD150^+$ fractions were analyzed. At the same time, 3×10^3 $GFP^+Ly5.1^+$ LSK cells were isolated from primary recipient mice and transplanted into lethally irradiated recipient mice (secondary BMT). The percentage of donor-derived GFP^+ cells in PB was also analyzed monthly. Sixteen weeks after the second BMT, the percentages of donor-derived cells in BM HSC fractions were analyzed in the same manner as the first BMT.

To evaluate the effect of the overexpression of mutant forms of Pot1a, LT-HSCs (8 week-old) were transduced with retrovirus expressing Pot1a, Pot1aΔOB, or Po1aΔTBD and transplanted into lethally irradiated recipient mice. After 5 month of BMT, the percentages of GFP^+ donor-derived cells were analyzed.

To analyze the function of Pot1a overexpression in the maintenance of HSC self-renewal in culture, Pot1a or control GFP-transduced $Ly5.1^+$ LSK cells (8 week-old) were cultured for 1-2 weeks in SF-O3 medium in the presence of 0.1% BSA, 100 ng ml^{-1} SCF, and 100 ng ml^{-1} TPO. After culture, GFP^+ LSK cells were transplanted into lethally irradiated recipient mice. Four months after BMT, the frequency of donor-derived GFP^+ cells in PB was analyzed by flow cytometry.

Evaluation of LTR activity of HSCs treated with MTM-POT1a

LSKCD41$^-$CD48$^-$CD150$^+$ cells (isolated from Ly5.1 mice) were cultured for 10 days in SF-O3 medium in the presence of 0.1% BSA, 100 ng ml^{-1} SCF, and 100 ng ml^{-1} TPO, with MTM-POT1a (350 ng ml^{-1}) or control MTM protein. The cultures were divided by transferring one-half of the cultured cells into fresh medium at day 7. After 10 days of culture, cells were collected and transplanted into lethally irradiated Ly5.2 recipient mice (first BMT). The percentage of donor-derived cells in PB was analyzed monthly. Sixteen weeks post-BMT, the percentages of donor-derived B, T, and GM cells in PB, and in BMMNC, LSK, and LSKCD41$^-$CD48$^-$CD150$^+$ fractions were analyzed. For the second BMT, BMMNCs (4×10^6 cells mouse^{-1}) were isolated from primary recipient mice and transplanted into lethally irradiated recipient mice. The percentage of donor-derived GFP$^+$ cells in PB was again analyzed monthly. Sixteen weeks after BMT, the percentages of donor-derived B, T, and GM cells in PB, and in BMMNCs, LSK, and LSKCD41$^-$CD48$^-$CD150$^+$ fractions were again analyzed.

To evaluate the effect of mutant forms of Pot1a proteins on LTR activity of HSCs, LT-HSCs were cultured with MTM-(wild type) Pot1a, MTM-POT1aΔOB, or MTM-Po1aΔTBD for 10 days and transplanted into lethally irradiated recipient mice. After 4 months of BMT, the percentage of donor-derived (Ly5.1$^+$) cells in PB was analyzed.

For the limiting dilution competitive BMT assay, LSKCD41$^-$CD48$^-$CD150$^+$ cells (from Ly5.1$^+$ mice) were cultured for 10 days in SF-O3 medium in the presence of 0.1% BSA, 100 ng ml^{-1} SCF, and 100 ng ml^{-1} TPO, with MTM-POT1a or control MTM. After culture, LSKCD41$^-$CD48$^-$CD150$^+$ cells were sorted and transplanted (20 or 50 cells mice^{-1}) into lethally irradiated Ly5.2 recipient mice. PB chimerism of >1.0% at 16 weeks after BMT was taken to verify long-term engraftment.

For the limiting dilution BMT assay of cultured human HSCs, hCB LT-HSCs (Lin^- $CD34^+CD38^-CD90^+CD45RA^-CD49f^+$ cells) were cultured for 9 days with MTM-POT1 or control MTM. After the culture, 5 x 10^3 or 2 x 10^4 $CD34^+$ cells were transplanted into irradiated (2.4 Gy) NOG mice.

Statistical analysis

Significant differences between groups were determined using 2-tailed Student's *t*-tests. Tukey's multiple comparison tests were used for multiple group comparisons. Significance of colocalization was assessed as described above. Frequency of LT-HSCs and statistical significance were determined using the ELDA software (http://bioinf.wehi.edu.au/software/elda/).

Data availability

The authors declare that all data supporting the findings of this study are available within the article or from the corresponding author upon reasonable request. Microarray data have been deposited in the GEO database under accession codes: GSE86386 and GSE85016.

References

1. Nijnik, A. *et al*. DNA repair is limiting for haematopoietic stem cells during ageing. *Nature* **447**, 686-690 (2007).
2. Rossi, D.J. *et al*. Deficiencies in DNA damage repair limit the function of haematopoietic stem cells with age. *Nature* **447**, 725-729 (2007).
3. Sperka, T., Wang, J. & Rudolph, K.L. DNA damage checkpoints in stem cells, ageing and cancer. *Nat Rev Mol Cell Biol* **13**, 579-590 (2012).
4. Wang, J. *et al*. A differentiation checkpoint limits hematopoietic stem cell self-renewal in response to DNA damage. *Cell* **148**, 1001-1014 (2012).
5. Flach, J. *et al*. Replication stress is a potent driver of functional decline in ageing haematopoietic stem cells. *Nature* **512**, 198-202 (2014).
6. Walter, D. *et al*. Exit from dormancy provokes DNA-damage-induced attrition in haematopoietic stem cells. *Nature* **520**, 549-552 (2015).
7. Hewitt, G. *et al*. Telomeres are favoured targets of a persistent DNA damage response in ageing and stress-induced senescence. *Nature communications* **3**, 708 (2012).
8. de Lange, T. How telomeres solve the end-protection problem. *Science* **326**, 948-952 (2009).
9. Vaziri, H. *et al*. Evidence for a mitotic clock in human hematopoietic stem cells: loss of telomeric DNA with age. *Proc Natl Acad Sci U S A* **91**, 9857-9860 (1994).
10. Lansdorp, P.M. Role of telomerase in hematopoietic stem cells. *Ann N Y Acad Sci* **1044**, 220-227 (2005).
11. de Lange, T. Shelterin: the protein complex that shapes and safeguards human telomeres. *Genes Dev* **19**, 2100-2110 (2005).
12. Palm, W. & de Lange, T. How shelterin protects mammalian telomeres. *Annu Rev Genet* **42**, 301-334 (2008).
13. Lei, M., Podell, E.R. & Cech, T.R. Structure of human POT1 bound to telomeric single-stranded DNA provides a model for chromosome end-protection. *Nature structural & molecular biology* **11**, 1223-1229 (2004).
14. Loayza, D. & De Lange, T. POT1 as a terminal transducer of TRF1 telomere length control. *Nature* **423**, 1013-1018 (2003).
15. Denchi, E.L. & de Lange, T. Protection of telomeres through independent control of ATM and ATR by TRF2 and POT1. *Nature* **448**, 1068-1071 (2007).
16. Choi, K.H. *et al*. The OB-fold domain 1 of human POT1 recognizes both telomeric and non-telomeric DNA motifs. *Biochimie* **115**, 17-27 (2015).
17. Hockemeyer, D., Daniels, J.P., Takai, H. & de Lange, T. Recent expansion of the telomeric complex in rodents: Two distinct POT1 proteins protect mouse telomeres. *Cell* **126**, 63-77 (2006).

18. Wu, L. *et al*. Pot1 deficiency initiates DNA damage checkpoint activation and aberrant homologous recombination at telomeres. *Cell* **126**, 49-62 (2006).
19. Hockemeyer, D., Palm, W., Wang, R.C., Couto, S.S. & de Lange, T. Engineered telomere degradation models dyskeratosis congenita. *Genes Dev* **22**, 1773-1785 (2008).
20. He, H. *et al*. Pot1b deletion and telomerase haploinsufficiency in mice initiate an ATR-dependent DNA damage response and elicit phenotypes resembling dyskeratosis congenita. *Mol Cell Biol* **29**, 229-240 (2009).
21. Jones, M. *et al*. Hematopoietic stem cells are acutely sensitive to Acd shelterin gene inactivation. *J Clin Invest* **124**, 353-366 (2014).
22. Wang, Y., Shen, M.F. & Chang, S. Essential roles for Pot1b in HSC self-renewal and survival. *Blood* **118**, 6068-6077 (2011).
23. Beier, F., Foronda, M., Martinez, P. & Blasco, M.A. Conditional TRF1 knockout in the hematopoietic compartment leads to bone marrow failure and recapitulates clinical features of dyskeratosis congenita. *Blood* **120**, 2990-3000 (2012).
24. Hockemeyer, D. *et al*. Telomere protection by mammalian Pot1 requires interaction with Tpp1. *Nature structural & molecular biology* **14**, 754-761 (2007).
25. Takai, H., Smogorzewska, A. & de Lange, T. DNA damage foci at dysfunctional telomeres. *Current biology : CB* **13**, 1549-1556 (2003).
26. Jiang, K. *et al*. Regulation of Chk1 includes chromatin association and 14-3-3 binding following phosphorylation on Ser-345. *J Biol Chem* **278**, 25207-25217 (2003).
27. Liu, Q. *et al*. Chk1 is an essential kinase that is regulated by Atr and required for the G(2)/M DNA damage checkpoint. *Genes Dev* **14**, 1448-1459 (2000).
28. Ito, K. *et al*. Regulation of oxidative stress by ATM is required for self-renewal of haematopoietic stem cells. *Nature* **431**, 997-1002 (2004).
29. Chen, C. *et al*. TSC-mTOR maintains quiescence and function of hematopoietic stem cells by repressing mitochondrial biogenesis and reactive oxygen species. *J Exp Med* **205**, 2397-2408 (2008).
30. Qian, P. *et al*. The Dlk1-Gtl2 Locus Preserves LT-HSC Function by Inhibiting the PI3K-mTOR Pathway to Restrict Mitochondrial Metabolism. *Cell Stem Cell* **18**, 214-228 (2016).
31. Hawiger, J. Noninvasive intracellular delivery of functional peptides and proteins. *Current opinion in chemical biology* **3**, 89-94 (1999).
32. Jo, D., Liu, D., Yao, S., Collins, R.D. & Hawiger, J. Intracellular protein therapy with SOCS3 inhibits inflammation and apoptosis. *Nat Med* **11**, 892-898 (2005).
33. Sakaue-Sawano, A. *et al*. Visualizing spatiotemporal dynamics of multicellular cell-cycle progression. *Cell* **132**, 487-498 (2008).
34. Notta, F. *et al*. Isolation of Single Human Hematopoietic Stem Cells Capable of Long-

693 Term Multilineage Engraftment. *Science* **333**, 218-221 (2011).
694 35. Suda, T., Takubo, K. & Semenza, G.L. Metabolic regulation of hematopoietic stem cells
695 in the hypoxic niche. *Cell Stem Cell* **9**, 298-310 (2011).
696 36. Takubo, K. *et al*. Regulation of glycolysis by Pdk functions as a metabolic checkpoint
697 for cell cycle quiescence in hematopoietic stem cells. *Cell Stem Cell* **12**, 49-61 (2013).
698 37. Ema, H., Takano, H., Sudo, K. & Nakauchi, H. In vitro self-renewal division of
699 hematopoietic stem cells. *J Exp Med* **192**, 1281-1288 (2000).
700 38. de Haan, G. *et al*. In vitro generation of long-term repopulating hematopoietic stem
701 cells by fibroblast growth factor-1. *Dev Cell* **4**, 241-251 (2003).
702 39. Walasek, M.A., van Os, R. & de Haan, G. Hematopoietic stem cell expansion:
703 challenges and opportunities. *Ann N Y Acad Sci* **1266**, 138-150 (2012).
704 40. Zhang, C.C. *et al*. Angiopoietin-like proteins stimulate ex vivo expansion of
705 hematopoietic stem cells. *Nat Med* **12**, 240-245 (2006).
706 41. Zheng, J. *et al*. Inhibitory receptors bind ANGPTLs and support blood stem cells and
707 leukaemia development. *Nature* **485**, 656-660 (2012).
708 42. Antonchuk, J., Sauvageau, G. & Humphries, R.K. HOXB4-induced expansion of adult
709 hematopoietic stem cells ex vivo. *Cell* **109**, 39-45 (2002).
710 43. Krosl, J. *et al*. In vitro expansion of hematopoietic stem cells by recombinant TAT-
711 HOXB4 protein. *Nat Med* **9**, 1428-1432 (2003).
712 44. Sauvageau, G. *et al*. Overexpression of HOXB4 in hematopoietic cells causes the
713 selective expansion of more primitive populations in vitro and in vivo. *Genes Dev* **9**,
714 1753-1765 (1995).
715 45. Goessling, W. *et al*. Prostaglandin E2 enhances human cord blood stem cell
716 xenotransplants and shows long-term safety in preclinical nonhuman primate transplant
717 models. *Cell Stem Cell* **8**, 445-458 (2011).
718 46. Boitano, A.E. *et al*. Aryl hydrocarbon receptor antagonists promote the expansion of
719 human hematopoietic stem cells. *Science* **329**, 1345-1348 (2010).
720 47. Fares, I. *et al*. Cord blood expansion. Pyrimidoindole derivatives are agonists of human
721 hematopoietic stem cell self-renewal. *Science* **345**, 1509-1512 (2014).
722 48. Costes, S.V. *et al*. Automatic and quantitative measurement of protein-protein
723 colocalization in live cells. *Biophys J* **86**, 3993-4003 (2004).
724 49. Dunn, K.W., Kamocka, M.M. & McDonald, J.H. A practical guide to evaluating
725 colocalization in biological microscopy. *American journal of physiology. Cell*
726 *physiology* **300**, C723-742 (2011).
727 50. Otsu, N. A threshold selection method from gray-level histograms. *Automatica* **11**, 23-
728 27 (1975).
729 51. Bolstad, B.M., Irizarry, R.A., Astrand, M. & Speed, T.P. A comparison of normalization

methods for high density oligonucleotide array data based on variance and bias. *Bioinformatics* **19**, 185-193 (2003).

Acknowledgements: This work was supported by the funding program for Next Generation World-Leading Researchers (NEXT Program), a Scientific Research (B) (General), a grant-in-aid for Young Scientists (A) and a Challenging Exploratory Research from the Ministry of Education, Culture, Sports, Science and Technology (MEXT) of Japan, Tokyo Biochemical Research funding, a research grant from the Astellas Foundation for research on metabolic disorders, The Sumitomo Foundation, SENSHIN Medical Research Foundation, Daiichi Sankyo Foundation of Life Science and the European Union's Seventh Framework Programme (FP7/2007-2013) under grant agreement no: 306240 (SyStemAge).

Author Contributions: K.H., and F.A. designed and performed experiments, and analyzed and interpreted data; Y.M.I. and H.T. participated in performing experiments; B.D.M. analyzed the data; Y.M. and S.H. provided the pET28a-MTM vector and helped to prepare the MTM protein; K.H., B.D.M., T.S. and F.A. wrote the paper

Conflict-of-interest disclosure: The authors have no competing financial interests to declare.

Figure Legends

Figure 1. Expression of Pot1a in HSPCs.

(a) Expression of *Pot1a* in: Lineage$^+$ (Lin$^+$) cells; Lin$^-$Kit$^+$Sca-1$^-$ (LKS$^-$) cells; LSKCD41$^+$CD48$^+$CD150$^-$ multipotent progenitor (MPP) cells; LSKCD41$^+$CD48$^+$CD150$^+$ cells (ST-HSCs); LSKCD41$^-$CD48$^-$CD150$^+$ cells (LT-HSCs) isolated from 8 week-old mice. Data are expressed as the mean ± SD (n = 4, *p < 0.01, **p < 0.05 by Tukey's test). Representative data from 2 independent experiments are shown. (b) Immunocytochemical staining of POT1 (red) in HSPCs. Nucleus is stained by TOTO3 (blue). Scale bar, 2 μm. (c) Relative area of POT1 immunofluorescent dots in HSPCs. Fluorescence images were analyzed with ImageJ. Data are expressed as the mean ± SD (n = 64: MPP, n = 67: ST-HSCs, n = 54: LT-HSCs, *p < 0.01 by Tukey's test). Representative data from 2 independent experiments are shown. (d) Immunoblot analysis of POT1 in Lin$^+$, Lin$^-$, LSKCD150$^-$, and LSKCD150$^+$ cells (left panel). Densitometry analysis of the immunoblot is shown in the right panel. Representative data from 2 independent experiments are shown. (e) Expression of *Pot1a* in 8, 60 and 90 week-old LT-HSCs. Data are expressed as the mean ± SD (n = 4, *p < 0.01 by Tukey's test). Representative data from 2 independent experiments are shown. (f) Immunocytochemical staining of POT1 (red) in LT-HSCs isolated from 8 and 90 week-old mice. Scale bar, 2 μm. (g) Relative area of POT1 immunofluorescent dots in LT-HSCs isolated from 8 and 90 week-old mice. Data are expressed as the mean ± SD (n = 146: 8-week-old, n = 180: 90-week-old, *p < 0.01 by *t*-test).

Figure 2. Overexpression of Pot1a enhances HSC proliferation activity.

(a-c) Control GFP or Pot1a-transduced LSK cells isolated from 8 week-old mice were cultured for 2 weeks and their ability to form colonies was analyzed. (a) Representative colonies from control GFP (left) and Pot1a-transduced LSK cells (right) after 2 weeks in vitro culture. Scale bar, 0.5 mm. (b) Number of CFU-Cs. (c) Number of HPP-CFCs. Data are expressed as the mean

± SD (n = 3, *p < 0.01 by *t*-test). (d, e) Control GFP or Pot1a-transduced LSK cells were clone-sorted and cultured for 2 weeks in SF-O3 medium supplemented with SCF (20 ng ml^{-1}), TPO (50 ng ml^{-1}), IL-3 (20 ng ml^{-1}) and EPO (1 U ml^{-1}). (d) Development of colonies from single cells after 2 weeks in vitro culture. (e) Number of colonies derived from single cells after 1-3 weeks in vitro culture. Each colony was classified into 3 categories by their size (<1 mm, ≥1 mm, ≥2 mm). Data are expressed as the mean ± SD (n = 3, *p < 0.01, **p < 0.05 by Tukey's test). (f) Control GFP or Pot1a-transduced 8 week-old LSK cells were cultured for 7–14 days. Subsequently, 5×10^3 GFP^+LSK cells were transplanted into lethally irradiated mice. The number of recipient mice that showed long-term reconstitution of donor cells (>1% of $GFP^+Ly5.1^+$ cells in PB) is shown.

Figure 3. Overexpression of Pot1a maintains HSC LTR activity.

(a, b) Results of primary BMT. (a) Percentage of donor-derived ($Ly5.1^+GFP^+$) cells in recipient mice PB, BM LSK and LT-HSCs 4 months after BMT. (b) Peripheral blood analysis of B, T, and myeloid cell lineages 4 months post BMT. Data are expressed as the mean ± SD (n = 5 $group^{-1}$, **p < 0.05 by *t*-test). Representative data from 2 independent experiments are shown. (c, d) Results of secondary BMT. (c) The percentage of donor-derived ($Ly5.1^+GFP^+$) cells in recipient mice PB, BM LSK and LT-HSCs 4 months post secondary BMT. (d) Peripheral blood analysis of B, T, and myeloid cell lineages 4 months post secondary BMT. Data are expressed as the mean ± SD (n = 5, *p < 0.01 by *t*-test). Representative data from 2 independent experiments are shown.

Figure 4. Pot1a prevents DDR in HSCs.

(a, b) Telomeric DDR in 8 week-old LSK cells upon Pot1a knockdown. (a) Immunocytochemical staining of TRF1 (green) and 53BP1 (red). Foci co-stained with TRF1

and 53BP1 were identified as TIFs. Nuclei were stained with TOTO3 (blue). Scale bar, 2 μm. (b) Frequency of TIFs per cell after 1 week of culture. Data are expressed as the mean ± SD (n = 100, *p < 0.01 by *t*-test). Representative data from three independent experiments are shown. (c-f) Telomeric DDR in donor derived control-GFP or Pot1a overexpressing 8 week-old LSK cells 4 months post BMT. (c) Immunocytochemical staining of TRF1 (green) and 53BP1 (red). Nuclei were stained with TOTO3 (blue). Scale bar, 2 μm. (d) Frequency of TIFs per cell. Data are expressed as the mean ± SD (n = 120, *p < 0.01 by *t*-test). Representative data from 3 independent experiments are shown. (e) Immunocytochemical staining of TRF1 (green) and RPA32 (red). (f) Immunocytochemical staining of TRF1 (green) and pChk1 (red). Scale bar, 2 μm. (g) Flow cytometric analysis of Chk1 and pChk1 in donor derived GFP^+ $LSKCD48^-$ $CD150^+$ cells after 5 months of 2nd BMT. Mean fluorescence intensity of Chk1 and pChk1 (left panels). Data are expressed as the mean ± SD (n = 3, *p < 0.01 by *t*-test). Representative FACS profiles of Chk1 and pChk1 in donor derived GFP^+ $LSKCD48^-CD150^+$ cells (right panels).

Figure 5. Effect of exogenous Pot1a on ROS production in LT-HSCs in culture.

(a) Schematic of the microarray analysis. (b) GSEA plots demonstrating enrichment levels of indicated gene sets in control control-GFP versus Pot1a-transduced LT-HSCs. NES, NOM P value, and FDR are indicated. (c) Schematic of the measurement of ROS in LT-HSCs. (d) Intracellular ROS levels in control-GFP (blue) and Pot1a-transduced (red) LT-HSCs. Representative FACS profiles of CellROX in GFP^+ LT-HSCs are shown. (e) Mean fluorescence level. Data are expressed as the mean ± SD (n = 5, *p < 0.01 by *t*-test). Representative data from 2 independent experiments are shown. (f) Relative mean fluorescence level of MitoSOX in the GFP^+ LT-HSCs on days 4, 7, and 11 of culture. Mean fluorescence level of MitoSOX in control-GFP transduced LT-HSCs was set to 1.0. Data are expressed as the mean ± SD (n = 6: day 7, n = 12: day 7, n = 3: day 11, *p < 0.01 by Tukey's test). (g) Schematic of the measurement of ROS

in LT-HSCs upon overexpression or knockdown of Pot1a. (h) Expression of *Mtor* and *Rptor* in Pot1a-overexpressing LT-HSCs. Data are expressed as the mean ± SD (n = 4, *p < 0.01 by *t*-test). (i) Expression of *Mtor* and *Rptor* in Pot1a knockdown LT-HSCs. Data are expressed as the mean ± SD (n = 4, *p < 0.01 by *t*-test).

Figure 6. Treatment with exogenous POT1 protein protects LT-HSCs in culture.

(a) Effect of MTM-POT1a on colony formation of HSCs. LT-HSCs (8 week-old) were cultured with MTM-POT1a for 2 weeks. After culture, Lin^- cells were isolated and re-cultured in MethoCult™ GF M3434 medium (200 cells $dish^{-1}$). Data are expressed as the mean ± SD (n = 3, *p < 0.01 by Tukey's test). Representative data from two independent experiments are shown. (b, c) LT-HSCs (8 week-old) were cultured with MTM-POT1a or control MTM protein. (b) Number of total cells and LT-HSCs on day 4, 7, and 10 of culture. Data are expressed as the mean ± SD (n = 6, *p < 0.01 by *t*-test). (c) Percentage of Annexin V^+PI^+ apoptotic cells in LT-HSCs on day 4, 7, and 10 of culture. Data are expressed as the mean ± SD (n = 6, *p < 0.01 by *t*-test). (d) LT-HSCs (8 week-old) were transduced with control shRNA or shPot1a-1. After 2 days of shRNA transduction, GFP^+LT-HSCs were re-sorted and cultured with MTM-POT1a or control MTM protein. After 1 week of culture, Annexin V assay was performed. Percentage of Annexin V^+PI^+ apoptotic cells in GFP^+LT-HSC fraction is shown. (n=3, **p < 0.05 by Tukey's test). (e) Immunocytochemical staining of TRF (green), 53BP1 (red), and TOTO3 (blue) in 8 week-old LT-HSCs cultured for 3 weeks (left). Frequencies of TIFs after 3 weeks of culture (right). Data are expressed as the mean ± SD (n = 80–100, *p < 0.01 by *t*-test). (f) Representative FACS profiles of 8 week-old LT-HSCs after 3 weeks of culture with control MTM protein or MTM-POT1a (left). Numbers of LSK cells and LT-HSCs after 3 week culture (starting from 2400 cells) are shown in right panels. Data are expressed as the mean ± SD (n = 3, *p < 0.01 by *t*-test). Representative data from 5 independent experiments are shown.

Figure 7. MTM-POT1a maintains self-renewal activity of HSCs.

(a) Results of primary BMT. Percentage of donor-derived ($Ly5.1^+$) cells in PB and LT-HSC fractions 4 months after BMT. (b) Frequency of donor cells in T, B, and myeloid cell fractions in PB 4 months post BMT. Data are expressed as the mean ± SD ($n = 5$ group^{-1}, *$p < 0.01$, **$p < 0.05$ by *t*-test). Representative data from 4 independent experiments are shown. (c) Results of secondary BMT. Percentage of donor-derived ($Ly5.1^+$) cells in PB and LT-HSC fractions 4 months post secondary BMT. (d) Frequency of donor cells in T, B, and myeloid cell fractions in PB 4 months post secondary BMT. Data are expressed as the mean ± SD ($n = 5$ group^{-1}, *$p < 0.01$ by *t*-test). Representative data from 4 independent experiments are shown. (e) Effect of mutant forms of POT1a in the regulation of LTR activity of HSCs. Percentage of donor-derived ($Ly5.1^+$) cells in PB 4 months after BMT is shown. Data are expressed as the mean ± SD ($n = 5$ group^{-1}, *$p < 0.01$ by Tukey's test). Representative data from 2 independent experiments are shown. (f) Effect of the overexpression of mutant forms of Pot1a on the maintenance of LTR activity of HSCs. Percentages of GFP^+ donor-derived cells in PB 5 months after BMT are shown. Data are expressed as the mean ± SD ($n = 5$ group^{-1}, *$p < 0.01$ by Tukey's test). Representative data from 2 independent experiments are shown. (g) Result of limiting dilution competitive BMT. A log-fraction plot of the limiting dilution model is shown. The slope of the line is the log-active cell fraction. The dotted lines give 95% confidence intervals (n = 24: control 20 cells, n = 21: control 50 cells, n = 23: MTM-POT1a 20 cells, n = 23: MTM-POT1a 50 cells). Competitive repopulation units are also shown.

Figure 8. MTM-POT1a improves aged HSC function.

(a) Schematic of the analysis of cell number and apoptotic fraction of 90 week-old LT-HSCs after culture with MTM-POT1a or control MTM protein. (b) Number of total cells and LT-

HSCs on days 4, 7, and 10 of culture. Data are expressed as the mean ± SD (n = 5: day 4, n = 6: day 7 and 10, **p < 0.05 by *t*-test). (c) Percentage of Annexin V^+PI^+ apoptotic cells in LT-HSC fraction on day 4, 7, and 10 of culture. Data are expressed as the mean ± SD (n = 6-8). (d, e) Effect of MTM-POT1a on reconstitution after BMT of young and aged LT-HSCs. 8 and 90 week-old LT-HSCs were cultured with MTM-POT1a or control MTM protein for 10 days and transplanted into lethally irradiated mice. (d) Percentages of donor-derived ($Ly5.1^+$) cells in PB and LT-HSCs 4 months after BMT are shown (n = 5 $group^{-1}$, *p < 0.01, **p<0.05 by Tukey's test). Representative data from 2 independent experiments are shown. (e) Percentage of T cells ($CD3^+$), B cells ($B220^+$), and myeloid ($Mac\text{-}1^+/Gr\text{-}1^+$) cells in donor derived cells in PB (n = 5 $group^{-1}$, *p < 0.01, **p<0.05 by Tukey's test). Representative data from 2 independent experiments are shown. (f) 60 week-old LT-HSCs were cultured with MTM-POT1a or control MTM protein for 3 days. After the culture, gene expression profiles were analyzed by microarray. GSEA plots demonstrating enrichment levels of indicated gene sets in control MTM protein treated cells versus MTM-POT1a treated cells. NES, NOM P value, and FDR are indicated.

Figure 9. POT1 prevents DDR in human HSC.

(a) Expression of POT1 in hCB $CD34^+$ cells and LT-HSCs (Lin^- $CD34^+CD38^-CD45RA^-CD90^+CD49f^+$). (b) hCB-derived LT-HSCs were cultured with MTM-POT1. After 10 days of culture, cells were isolated and re-cultured in methylcellulose medium (200 cells $dish^{-1}$). The number of CFU-C and HPP-CFC (>1.0 mm, >2.0 mm) are shown. Data are expressed as the mean ± SD (n = 3, *p < 0.01 by *t*-test). Representative data from 3 independent experiments are shown. (c, d) hCB LT-HSCs were cultured for 10 days with control MTM protein or MTM-POT1. After 10 days of culture, LT-HSCs were re-isolated and number of TIF was examined. (c) Immunocytochemical staining of TRF1 (green), 53BP1 (red),

and TOTO3 (blue). Scale bar, 2 μm (left). Frequencies of TIFs after 10 days of culture (right). Data are expressed as the mean ± SD (n = 100: control, n = 100: MTM-POT1, *p < 0.01 by *t*-test). Representative data from 2 independent experiments are shown. (d) Immunocytochemical staining of TRF1 (green), RPA32 (red), and TOTO3 (blue). Scale bar, 2 μm (left). Frequencies of TIFs after 10 days of culture (right). Data are expressed as the mean ± SD (n = 110–120: control, n = 110: MTM-POT1, *p < 0.01 by *t*-test). Representative data from 2 independent experiments are shown. (e-g)

Figure 10. POT1 maintains self-renewal activity of human HSCs.

hCB-derived LT-HSCs (200 cells well^{-1}) were cultured for 10 days with or without MTM-POT1. (a) Number of total cells (left) and Lin$^-$CD34$^+$CD38$^-$CD45RA$^-$CD90$^+$ cells on day 7 and 10 of culture. Data are expressed as the mean ± SD (n = 10, *p < 0.01 by *t*-test). (b) Representative FACS profiles of CD90 and CD45RA in Lin$^-$CD34$^+$CD38$^-$CD49f$^+$ cells (left) and the expression of CD49f in the Lin$^-$CD34$^+$CD38$^-$CD45RA$^-$CD90$^+$ fraction (right). (c) Percentage of Annexin V$^+$PI$^+$ apoptotic cells in Lin$^-$CD34$^+$CD38$^-$CD45RA$^-$CD90$^+$ cells on day 7 and 10 of culture. Data are expressed as the mean ± SD (n = 11: day 7, n = 9: day 10). (d) LT-HSCs isolated from hBM (200 cells well^{-1}) were cultured for 10 days with or without MTM-POT1 (50 ng ml^{-1}). Number of total cells, CD34$^+$CD38$^-$ cells, and LT-HSCs after culture are shown. Data are expressed as the mean ± SD (n = 3, *p < 0.01, **p < 0.05 by *t*-test). Representative data from two independent experiments are shown. (e) Result of limiting dilution BMT. A log-fraction plot of the limiting dilution model is shown. The slope of the line is the log-active cell fraction. The dotted lines give 95% confidence intervals (n = 5). The data point with zero negative response at dose 20,000 is represented by a downward-pointing triangle. Estimated numbers of repopulating cells are also shown.

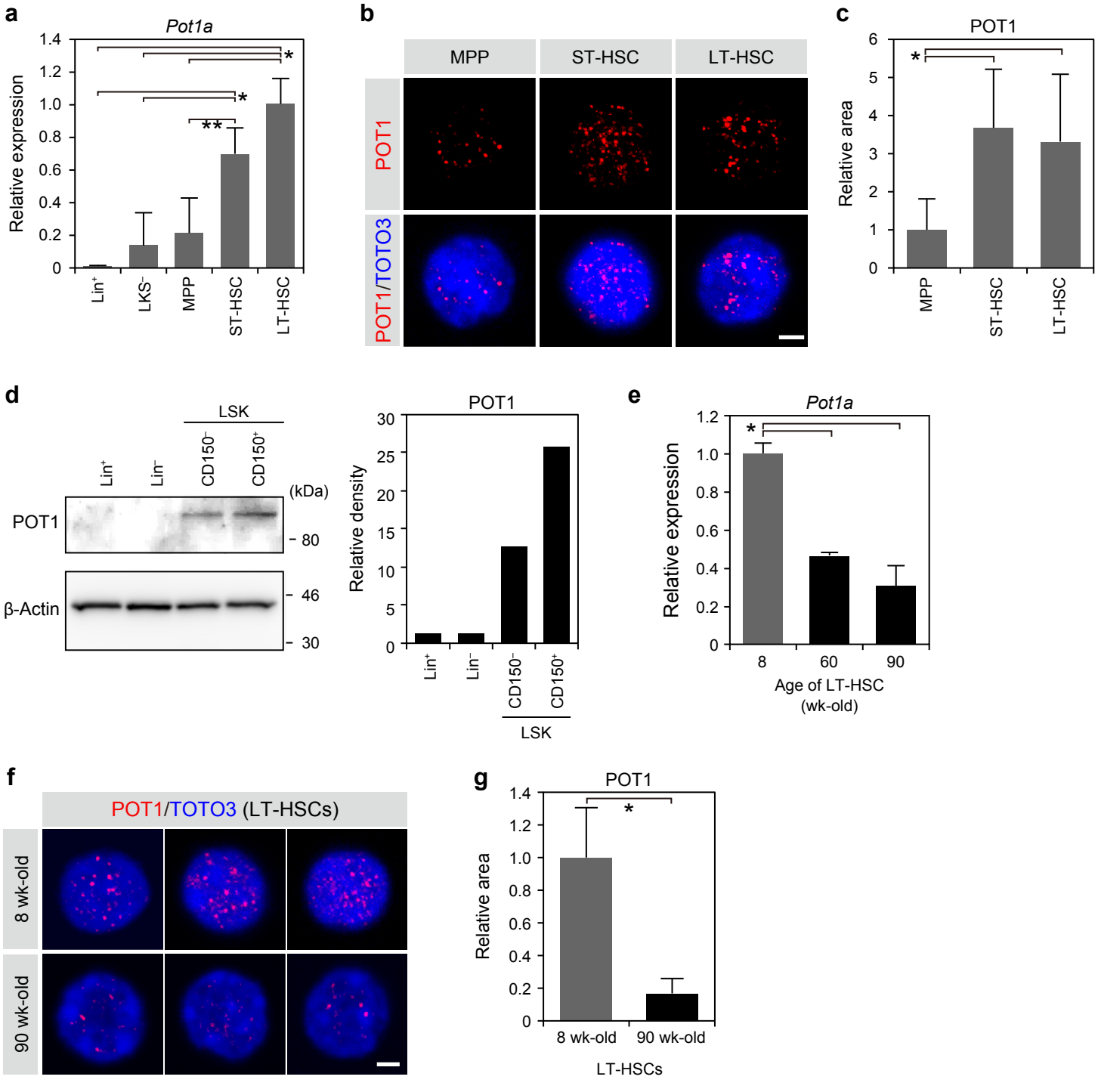

Figure 1R. Hosokawa et al.

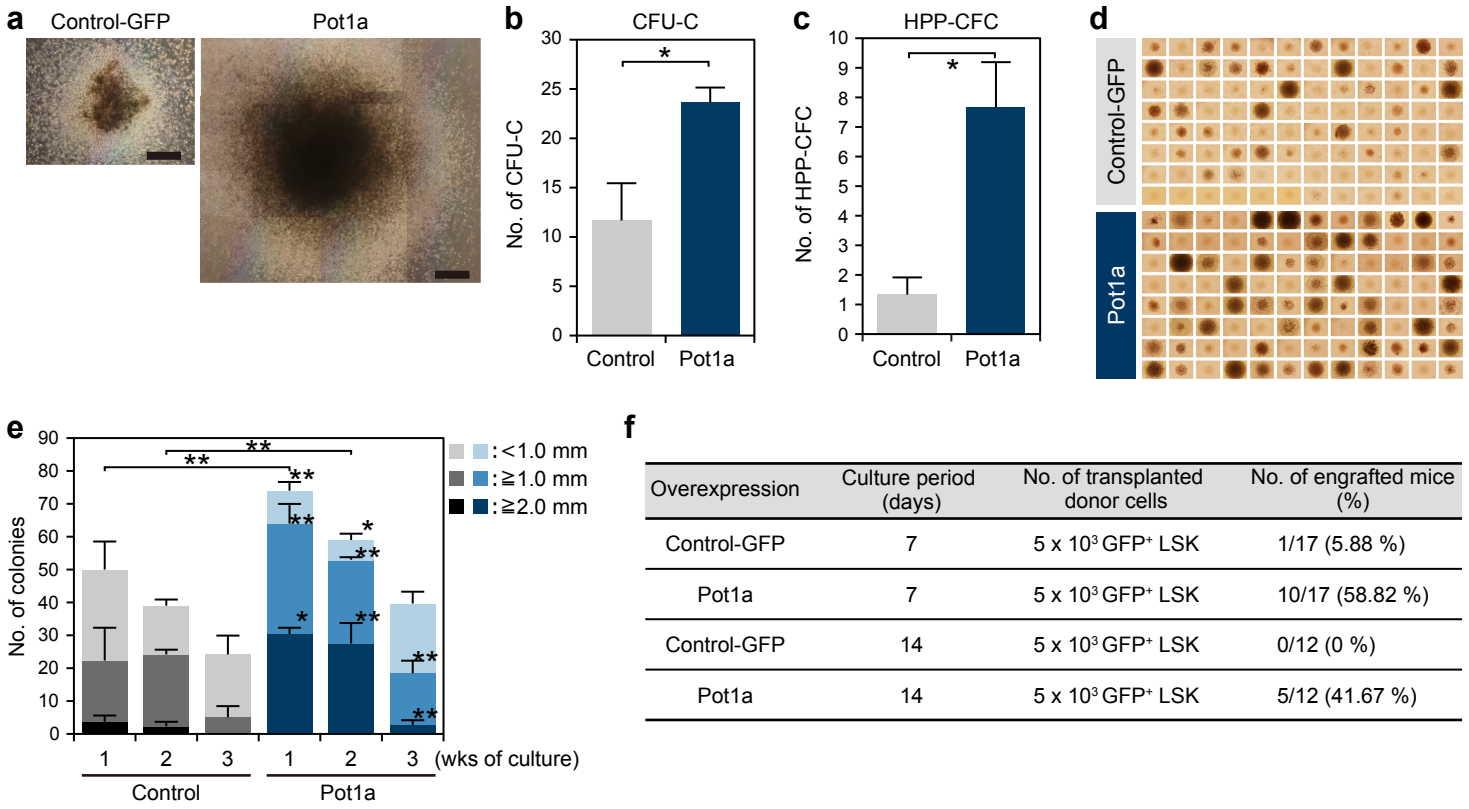

f

Overexpression	Culture period (days)	No. of transplanted donor cells	No. of engrafted mice (%)
Control-GFP	7	5 x 10^3 GFP^+ LSK	1/17 (5.88 %)
Pot1a	7	5 x 10^3 GFP^+ LSK	10/17 (58.82 %)
Control-GFP	14	5 x 10^3 GFP^+ LSK	0/12 (0 %)
Pot1a	14	5 x 10^3 GFP^+ LSK	5/12 (41.67 %)

Figure 2R. Hosokawa et al.

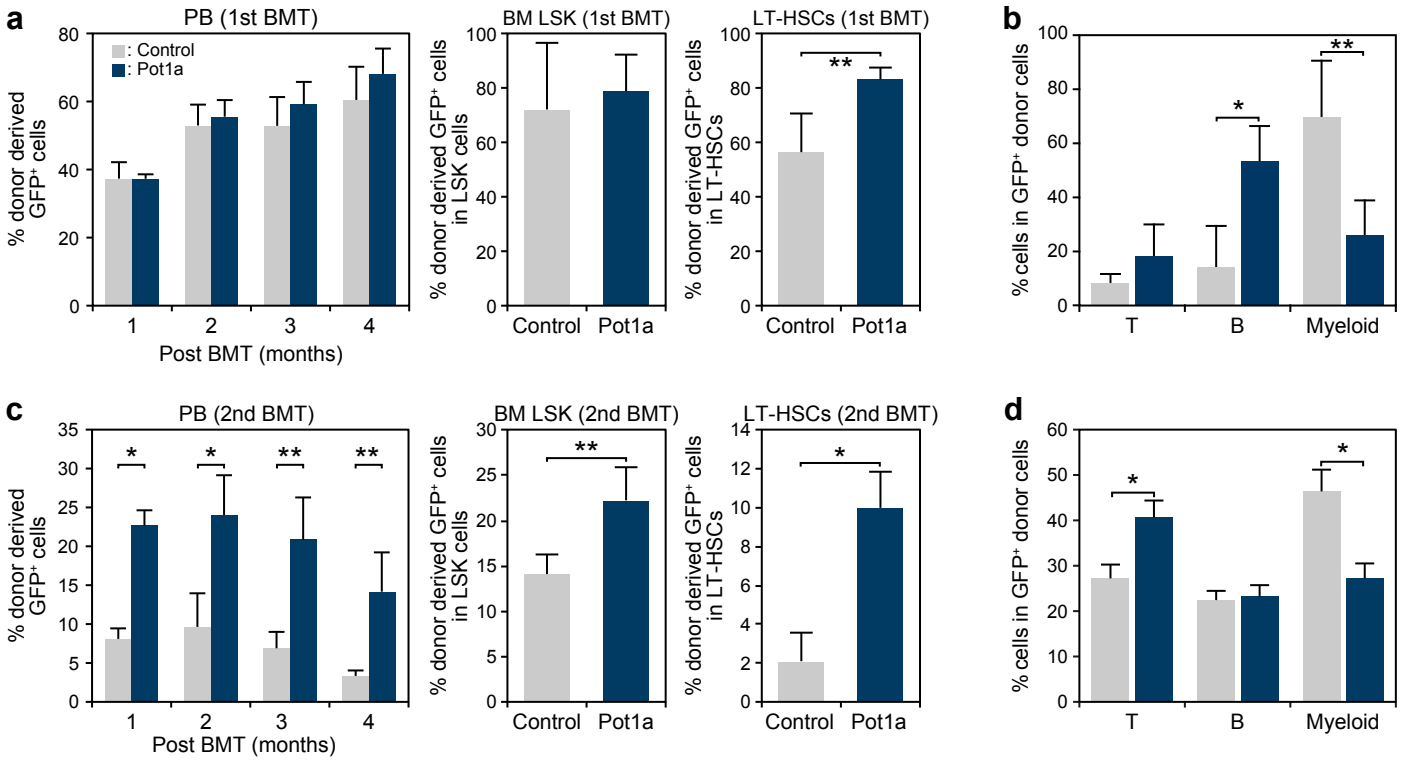

Figure 3R. Hosokawa et al.

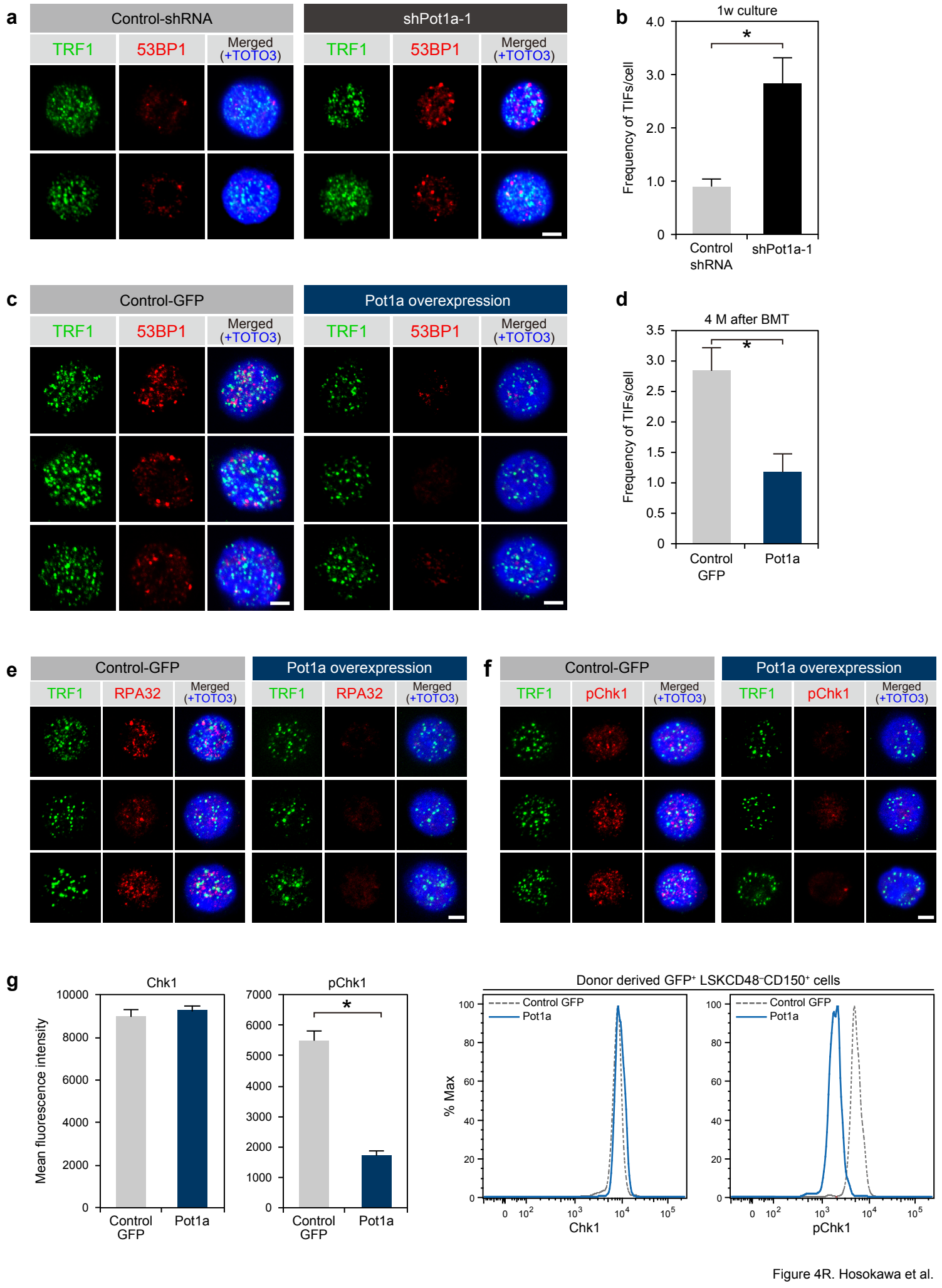

Figure 4R. Hosokawa et al.

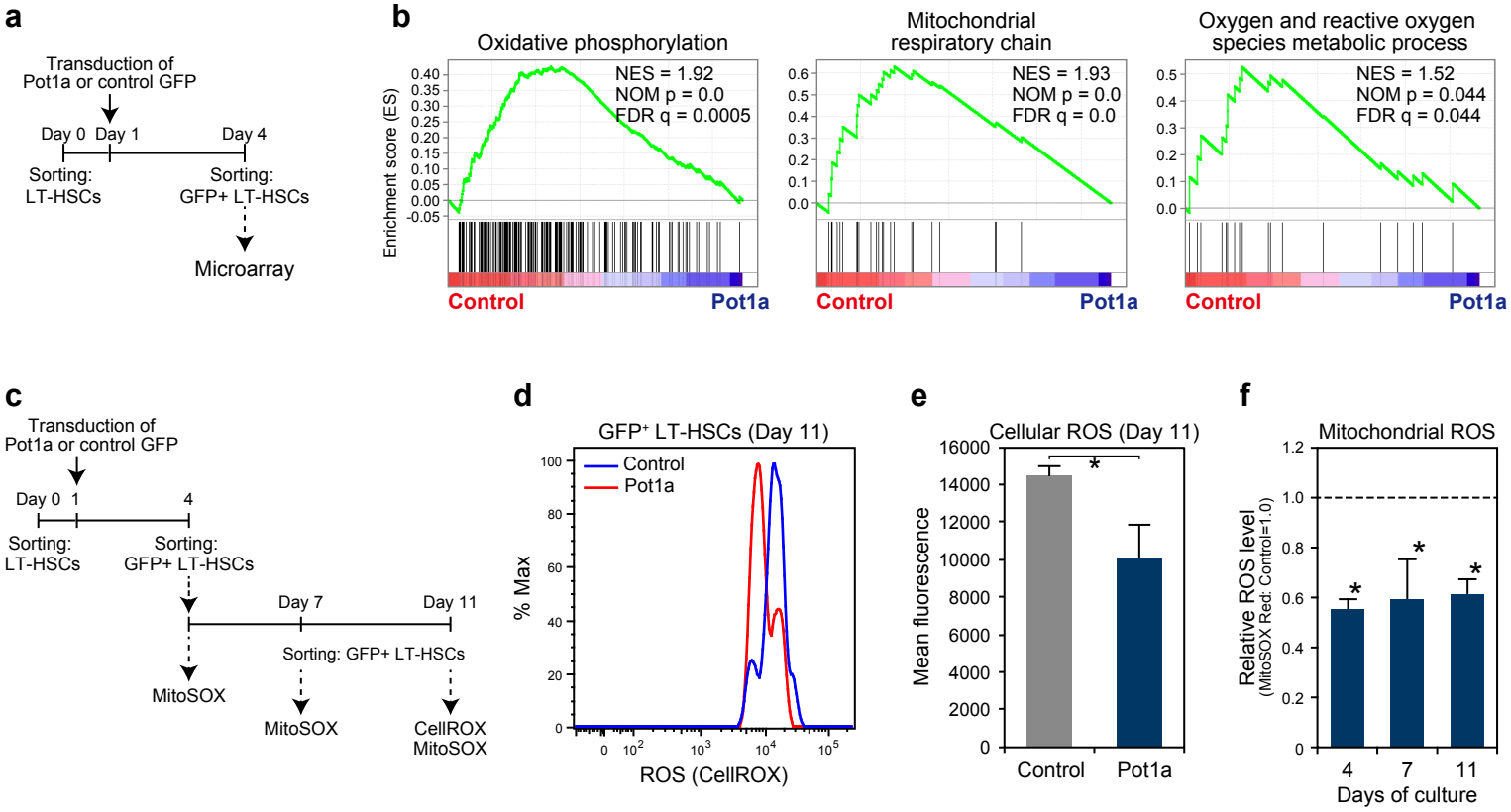

Figure 5R. Hosokawa et al.

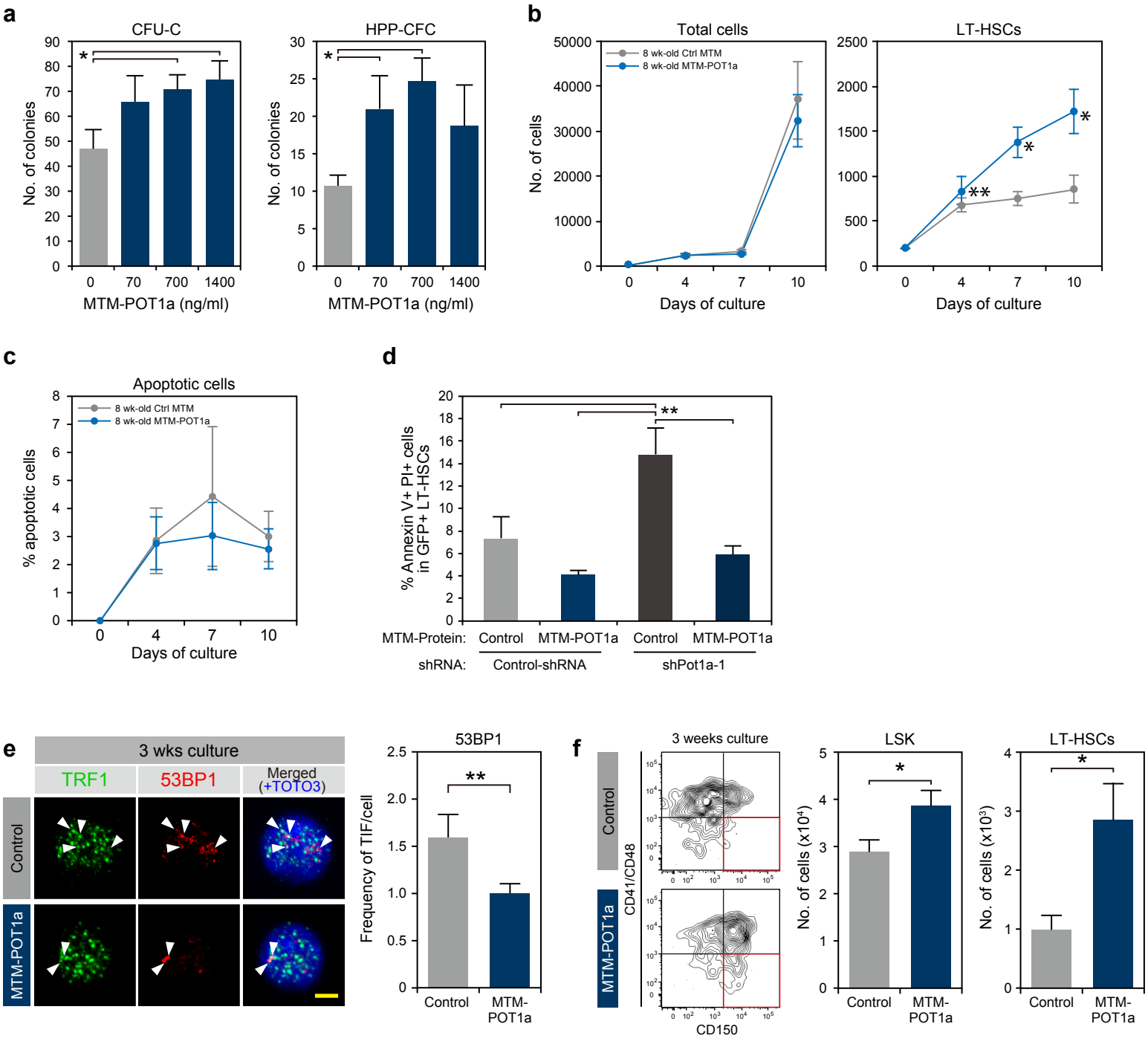

Figure 6R. Hosokawa et al.

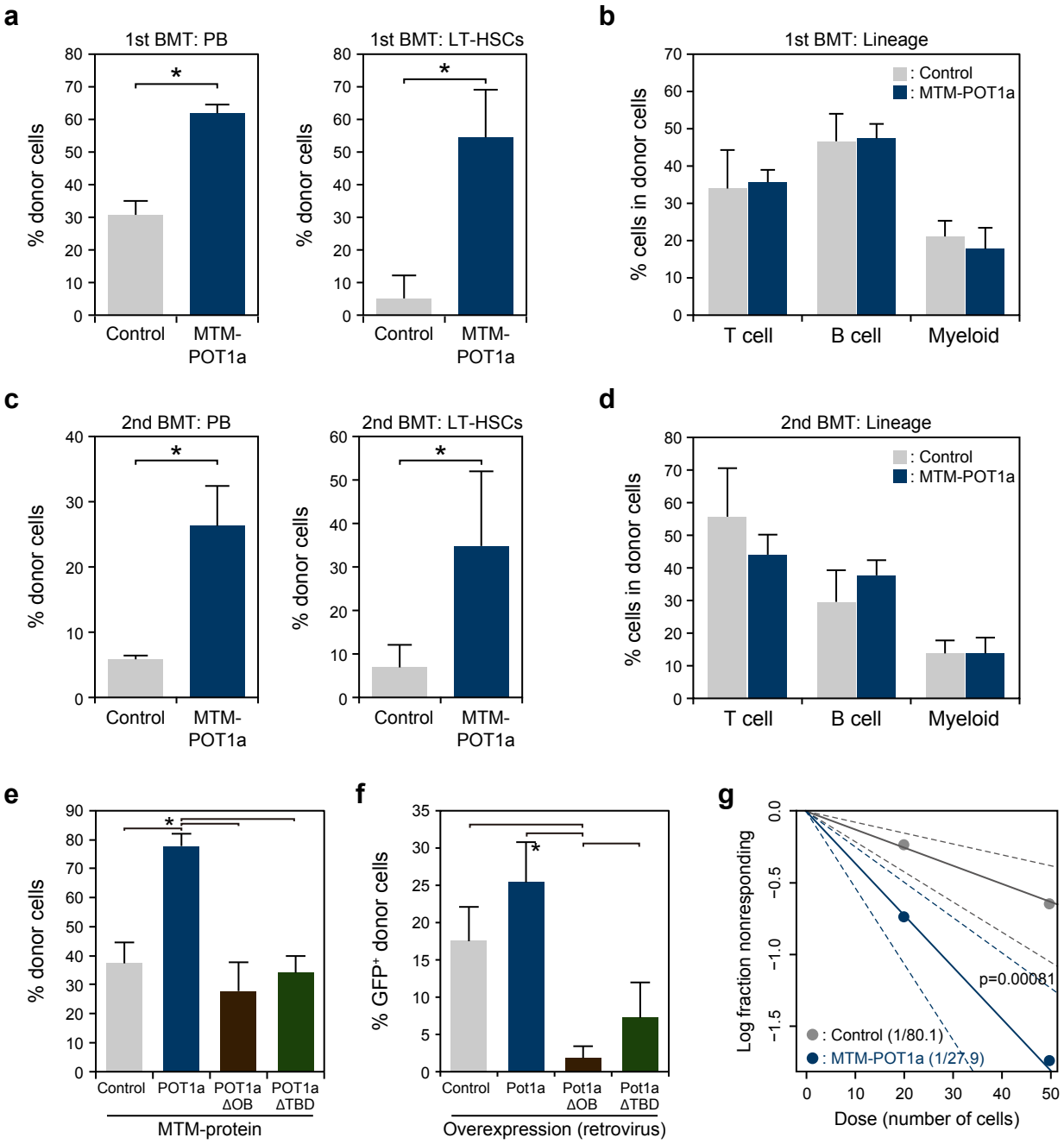

Figure 7R. Hosokawa et al.

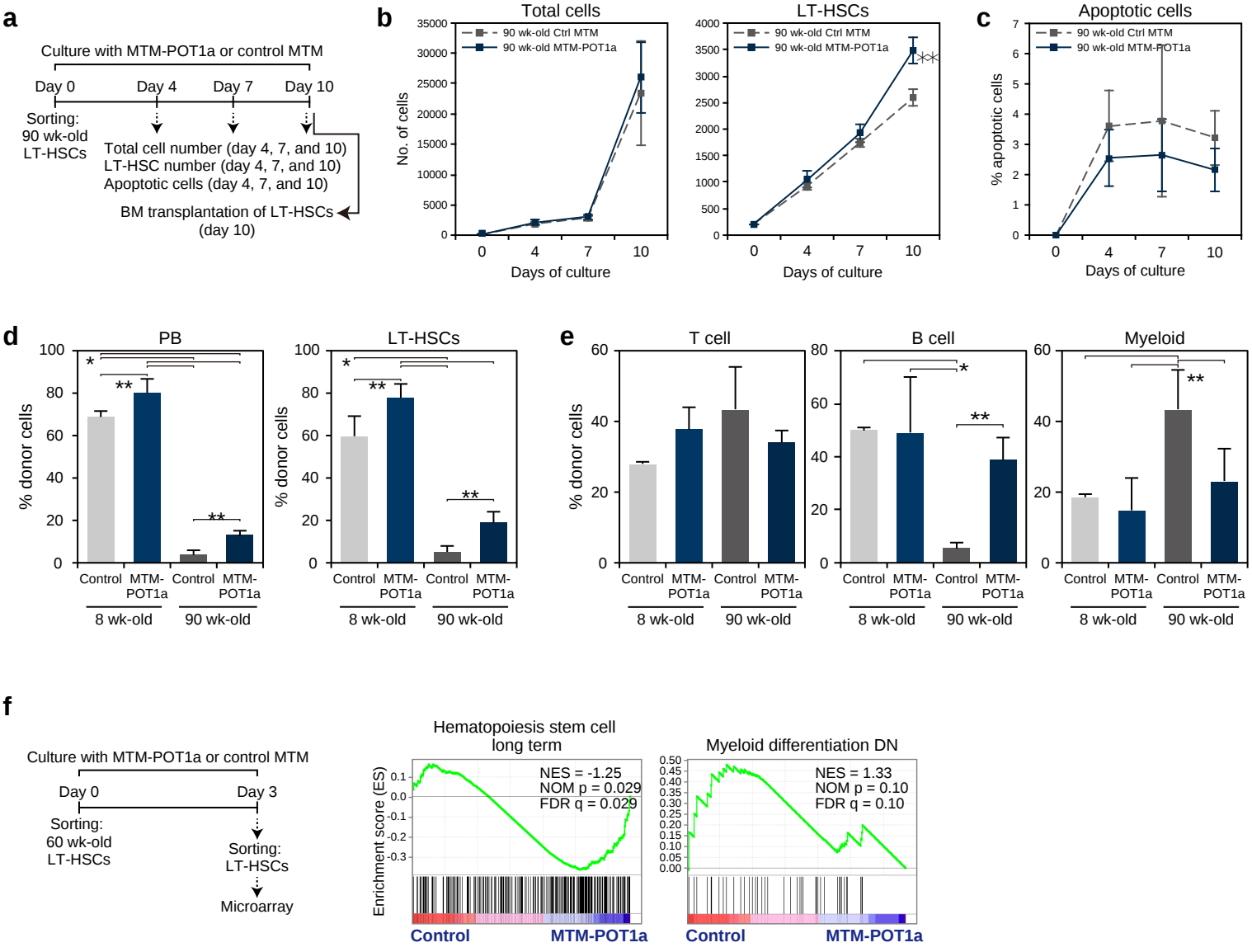

Figure 8R. Hosokawa et al.

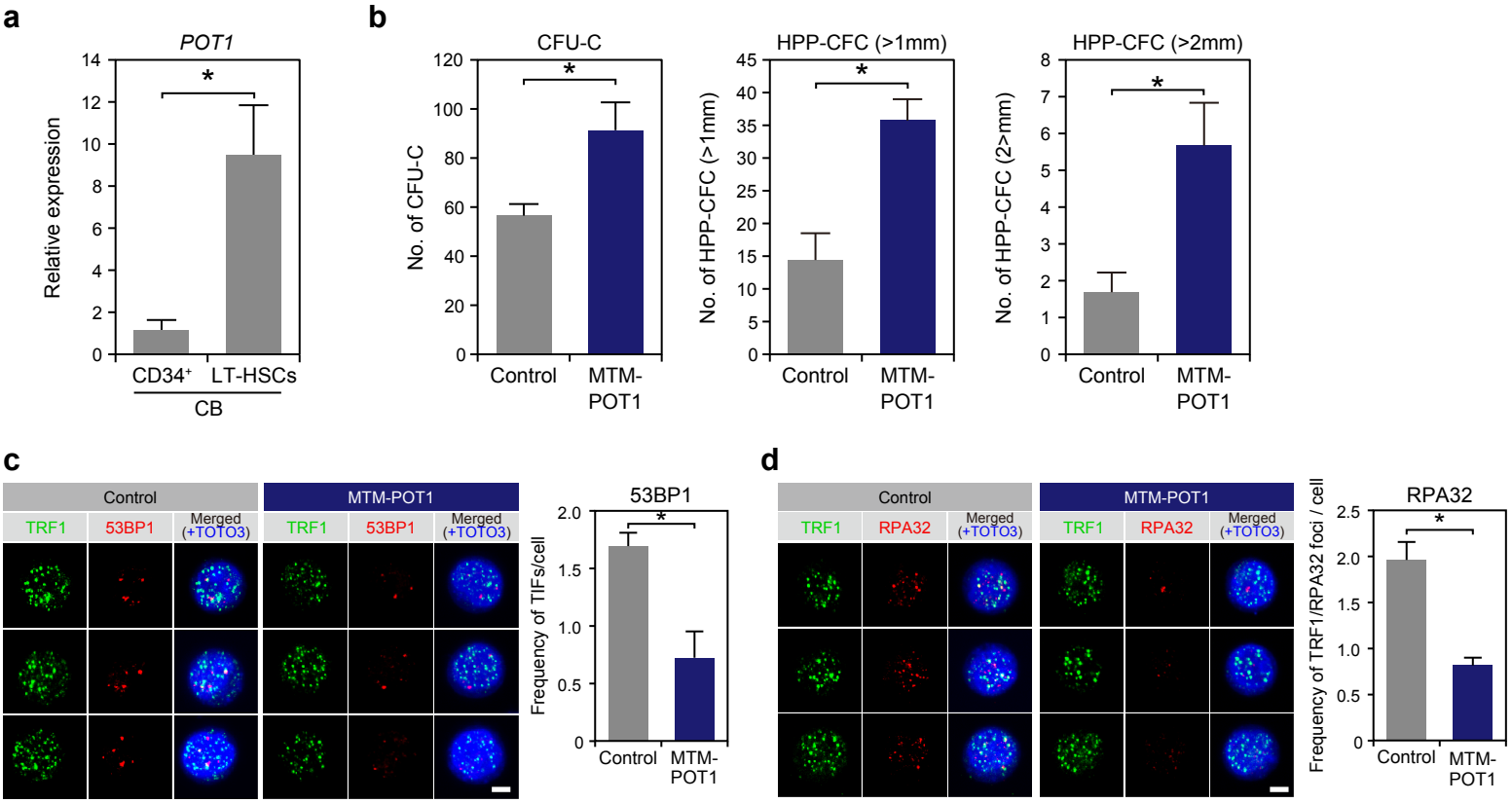

Figure 9R. Hosokawa et al.

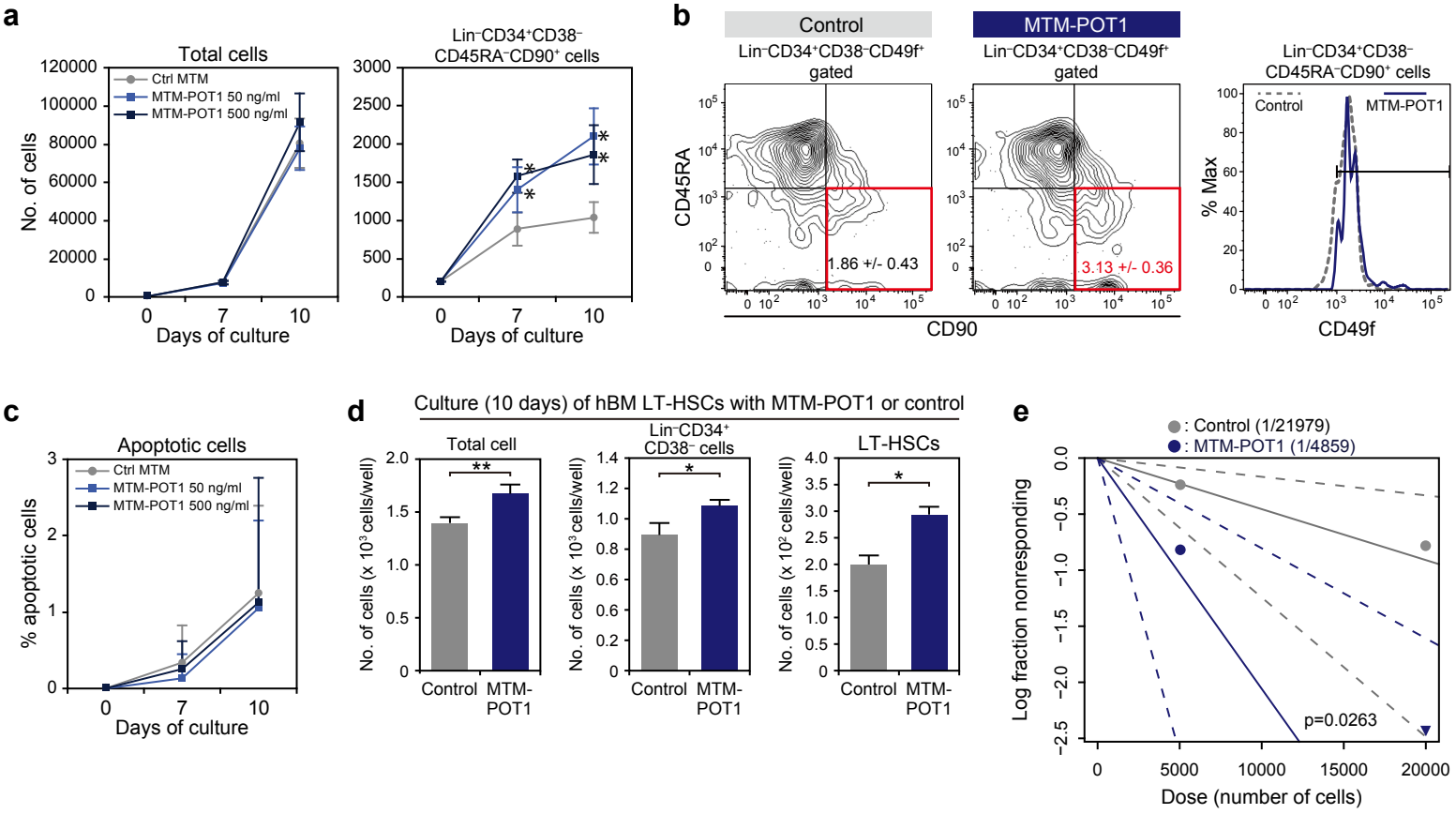

Figure 10R. Hosokawa et al.

Supplementary Table 1. Result of image analysis

			COLOCALIZATION OF GREEN CHANNEL WITH RED						COLOCALIZATION OF RED CHANNEL WITH GREEN					
	STAINING		MEAN		SD				MEAN		SD			
Samples	GREEN	RED	observed	randomized	observed	randomized	p-value	Welch's t-test p-value	observed	randomized	observed	randomized	p-value	Welch's t-test p-value
8 week-old HSCs	TRF1	53BP1	0.4661	0.3681	0.0525	0.0516	0.0153	<0.0001	0.5783	0.4533	0.048	0.0519	0.0102	<0.0001
90 week-old HSCs	TRF1	53BP1	0.1787	0.1148	0.0306	0.0246	0.0063	<0.0001	0.6255	0.4137	0.0588	0.0635	0.0044	<0.0001
10 days cultured 8 week-old HSCs/Control	TRF1	53BP1	0.7653	0.6533	0.0273	0.0318	0.0002	<0.0001	0.2244	0.1834	0.0156	0.0151	0.0002	<0.0001
10 days cultured 8 week-old HSCs/MTM-POT1a treated	TRF1	53BP1	0.6012	0.4609	0.0321	0.0337	<0.0001	<0.0001	0.2069	0.1454	0.0172	0.014	<0.0001	<0.0001
10 days cultured 90 week-old HSCs/Control	TRF1	53BP1	0.5819	0.5078	0.029	0.0286	0.0064	<0.0001	0.2524	0.213	0.0168	0.0161	0.0045	<0.0001
10 days cultured 90 week-old HSCs/MTM-POT1a treated	TRF1	53BP1	0.7512	0.6388	0.0231	0.028	<0.0001	<0.0001	0.2442	0.2009	0.0136	0.0124	<0.0001	<0.0001
3 week cultured 8 week-old HSCs/Control	TRF1	53BP1	0.4991	0.3198	0.0327	0.0321	<0.0001	<0.0001	0.4519	0.2893	0.0262	0.0265	<0.0001	<0.0001
3 week cultured 8 week-old HSCs/MTM-POT1a treated	TRF1	53BP1	0.5338	0.348	0.0405	0.041	<0.0001	<0.0001	0.3197	0.2071	0.0282	0.026	<0.0001	<0.0001
Control-shRNA transduced HSCs	TRF1	53BP1	0.2913	0.24	0.0578	0.0558	0.1653	<0.0001	0.4524	0.3741	0.0685	0.07	0.171	<0.0001
shPot1a transduced HSCs	TRF1	53BP1	0.2486	0.2009	0.0576	0.0532	0.1966	<0.0001	0.3444	0.2786	0.0671	0.0636	0.2014	<0.0001
Control GFP transduced HSCs /4M post BMT	TRF1	53BP1	0.5822	0.4229	0.1305	0.1353	0.1633	<0.0001	0.1326	0.0949	0.0442	0.0391	0.1785	<0.0001
Pot1a transduced HSCs /4M post BMT	TRF1	53BP1	0.6963	0.5256	0.1352	0.1525	0.1645	<0.0001	0.135	0.0951	0.0563	0.0426	0.1847	<0.0001
10 days cultured human CB HSCs /Control	TRF1	53BP1	0.509	0.4368	0.0358	0.0352	0.0092	<0.0001	0.4992	0.4229	0.0313	0.0313	0.0081	<0.0001
10 days cultured human CB HSCs /MTM-hPOT1 treated	TRF1	53BP1	0.4704	0.3174	0.0357	0.0342	<0.0001	<0.0001	0.3613	0.2495	0.0306	0.0281	0.0007	<0.0001
10 days cultured human CB HSCs /Control	TRF1	RPA32	0.3642	0.228	0.0322	0.0284	0.0001	<0.0001	0.3995	0.246	0.033	0.0287	<0.0001	<0.0001
10 days cultured human CB HSCs /MTM-hPOT1 treated	TRF1	RPA32	0.1494	0.1045	0.0217	0.018	0.0061	<0.0001	0.5428	0.4475	0.0552	0.0541	0.0906	<0.0001

Supplementary Table 2. TaqMan® Gene Expression Assay Mixes for Q-PCR analysis

Gene name	Gene symbol	Assay ID
Acd (Tpp1)	*Acd*	Mm01247801_g1
Ataxia telangiectasia mutated homolog	*Atm*	Mm01177457_m1
BCL2-associated agonist of cell death	*Bad*	Mm00432042_m1
BCL2-antagonist/killer 1	*Bak1*	Mm00432045_m1
BCL2-associated X protein	*Bax*	Mm00432050_m1
BCL2 binding component 3 (PUMA)	*Bbc3*	Mm00519268_m1
B cell leukemia/lymphoma 2	*Bcl2*	Mm00477631_m1
Bmi1 polycomb ring finger oncogene	*Bmi1*	Mm00776122_gH
CD34 antigen	*Cd34*	Mm00519283_m1
CD48 antigen	*Cd48*	Mm00455932_m1
Cyclin-dependent kinase inhibitor 1A (P21)	*Cdkn1a*	Mm00432448_m1
Cyclin-dependent kinase inhibitor 1C (P57)	*Cdkn1c*	Mm01272135_g1
Colony stimulating factor 1 receptor	*Csf1r*	Mm00432689_m1
Colony stimulating factor 3 receptor	*Csf3r*	Mm00432735_m1
Cyclin-dependent kinase inhibitor 2A (Cdkn2a), transcript variant 1	*p19Arf*	Custom*
Cyclin-dependent kinase inhibitor 2A (Cdkn2a), transcript variant 2	*p16Ink4a*	Custom**
Chemokine (C-X-C motif) receptor 4	*Cxcr4*	Mm01292123_m1
Enhancer of zeste homolog 2	*Ezh2*	Mm00468464_m1
FMS-like tyrosine kinase 3	*Flt3*	Mm00438996_m1
Forkhead box O1	*Foxo1*	Mm00490672_m1
Forkhead box O3	*Foxo3*	Mm01185722_m1
GATA binding protein 2	*Gata2*	Mm00492300_m1
Hairy and enhancer of split 1	*Hes1*	Mm01342805_m1
Homeobox B4	*Hoxb4*	Mm00657964_m1
Interferon regulatory factor 8	*Irf8*	Mm00492567_m1
MDS1 and EVI1 complex locus (Evi1)	*Mecom* (*Evi1*)	Mm00514814_m1
Myeloproliferative leukemia virus oncogene	*Mpl*	Mm00440310_m1
Myelocytomatosis oncogene	*Myc*	Mm00487803_m1

v-myc myelocytomatosis viral related oncogene, neuroblastoma derived	*Mycn*	Mm00627179_m1
Necdin	*Ndn*	Mm02524479_s1
Protection of telomeres 1A	*Pot1a*	Mm00505816_m1
Protection of telomeres 1B	*Pot1b*	Mm01278790_m1
Protein C receptor, endothelial	*Procr*	Mm00440992_m1
Selectin, platelet	*Selp*	Mm00441295_m1
Signaling lymphocytic activation molecule family member 1	*Slamf1*	Mm00443316_m1
T cell acute lymphocytic leukemia 1	*Tal1*	Mm00441665_m1
Endothelial-specific receptor tyrosine kinase (Tie2)	*Tek*	Mm00443242_m1
Telomerase RNA component	*Terc*	Mm01261365_s1
Telomeric repeat binding factor 1	*Terf1*	Mm00436923_m1
Telomeric repeat binding factor 2	*Terf2*	Mm01253555_m1
Telomeric repeat binding factor 2, interacting protein (Rap1)	*Terf2ip* (*Rap1*)	Mm01243676_m1
Telomerase reverse transcriptase	*Tert*	Mm01352136_m1
Terf1 (TRF1)-interacting nuclear factor 2	*Tinf2*	Mm00461166_g1
Transformation related protein 53	*Trp53*	Mm00441964_g1
Mechanistic target of rapamycin (serine/threonine kinase)	*Mtor*	Mm00444968_m1
regulatory associated protein of MTOR, complex 1	*Rptor*	Mm01242613_m1
Mouse ACTB (actin, beta) endogenous control	*Actb*	4352933E
Protection of telomeres 1 (human POT1)	*POT1*	Hs00209984_m1
Human ACTB (actin, beta)	*ACTB*	Hs01060665_g1

Supplementary Table 3. Primer and probe sequence for p16Ink4a and p19Arf

p19Arf	Forward	GTCACACGACTGGGCGATT
	Reverse	CAGTCTGTCTGCAGCGGACTC
	Probe	FAM-CACTGAATCTCCGCGAGG-MGB
p16Ink4a	Forward	GGGTTTTCTTGGTGAAGTTCGT
	Reverse	AAGATCCTCTCTAGCCTCAACAACA
	Probe	FAM-ACAGCGAGCTGCGCT-MGB

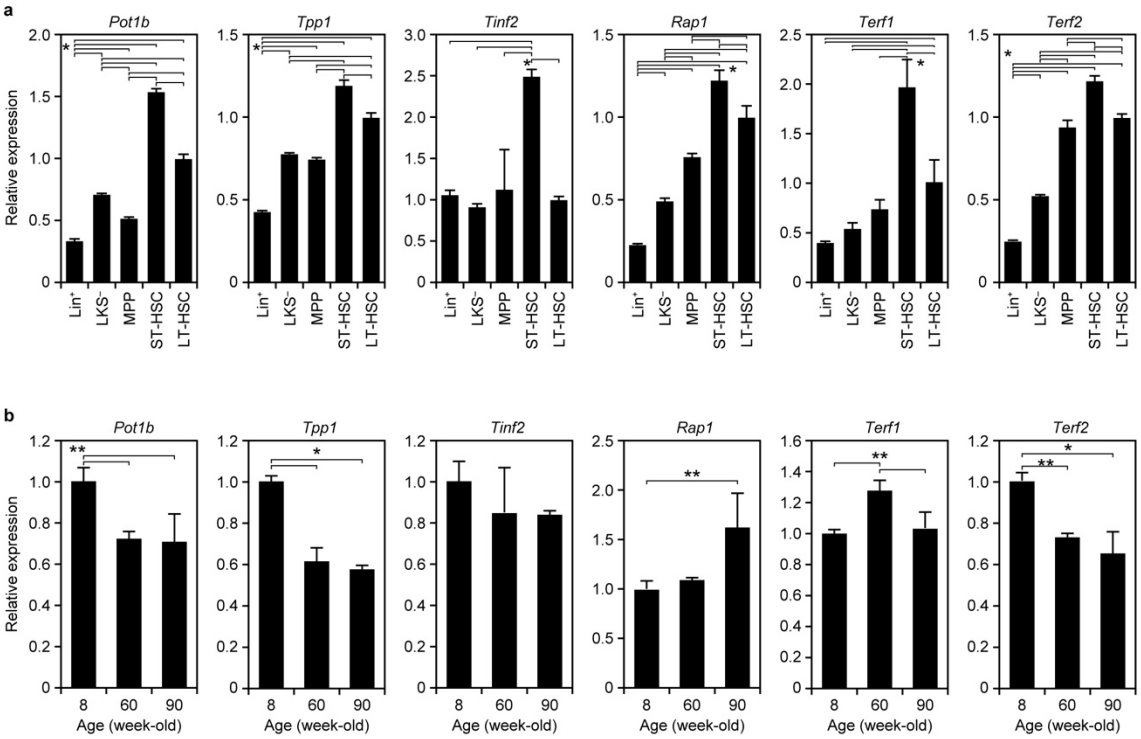

Supplementary Figure 1. Expression of shelterin components in fractionated hematopoietic cells

(a) Expression of *Pot1b*, *Tpp1*, *Tinf2*, *Rap1*, *Terf1*, and *Terf2* in fractionated hematopoietic cells isolated from 8 week-old mice. Lin^+, $lineage^+$ cells; LKS^- cells, $Lin^-Kit^+Sca\text{-}1^-$ cells; MPP, $LSKCD41^+CD48^+CD150^-$ cells; $LSKCD41^+CD48^+CD150^+$ ST-HSCs; $LSKCD41^-CD48^-CD150^+$ LT-HSCs. Data are expressed as the mean ± SD (n = 4, *p < 0.05 by Tukey's test). Representative data from 3 independent experiments are shown. (b) Expression of *Pot1b*, *Tpp1*, *Tinf2*, *Rap1*, *Terf1*, and *Terf2* in 8, 60 and 90 week-old LT-HSCs. Data are expressed as the mean ± SD (n = 4, *p < 0.01, **p < 0.05 by Tukey's test). Representative data from two independent experiments are shown.

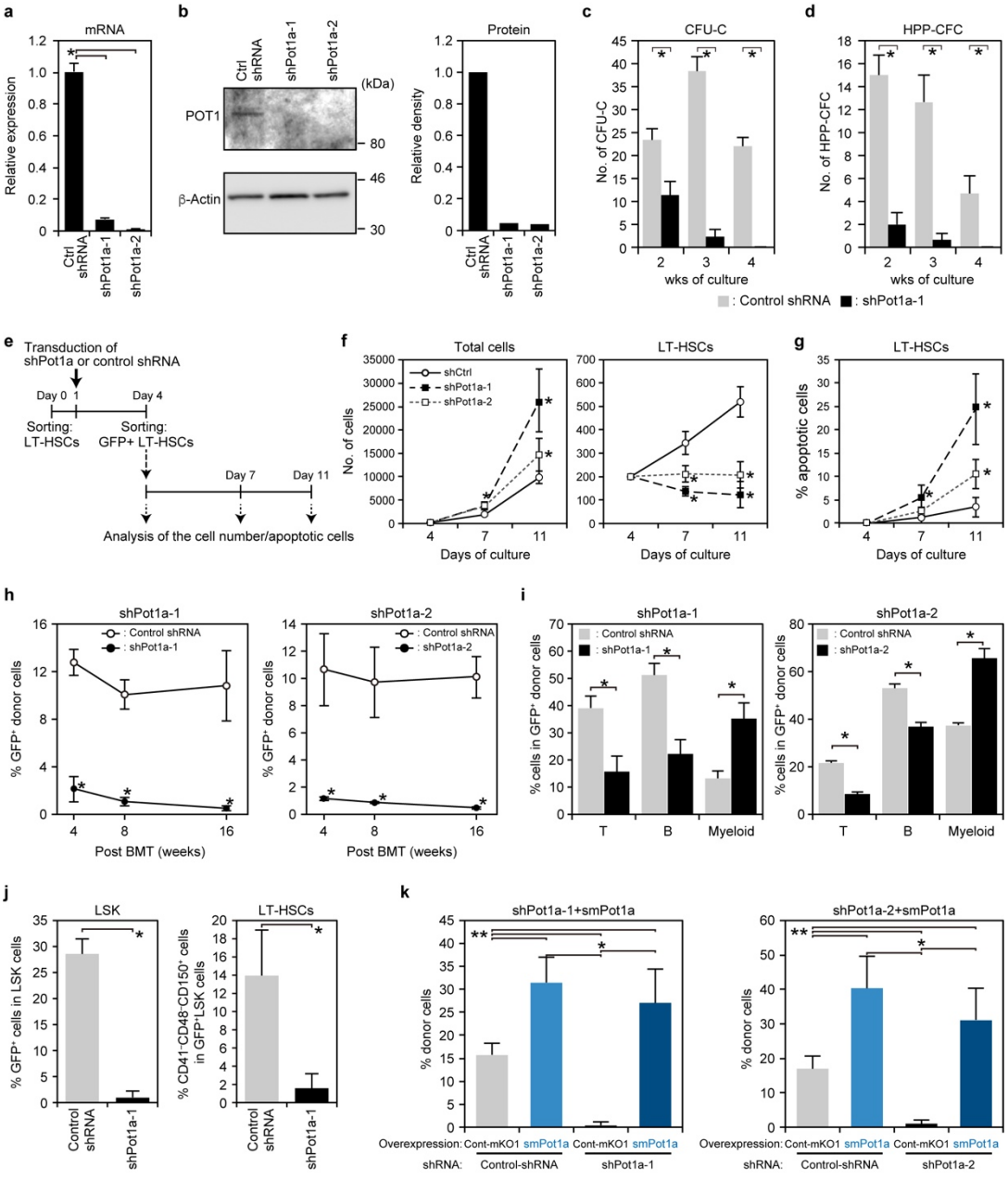

Supplementary Figure 2. Knockdown of Pot1a impairs HSC function.

(a, b) Efficiency of the knockdown of Pot1a. LT-HSCs (8 week-old) were transduced control shRNA, shPot1a-1 and -2. After 2 days of transduction, GFP^+ LT-HSCs cells were collected the expression of Pot1a mRNA and POT1 protein was analyzed. (a) Q-PCR analysis of the expression of *Pot1a*. Data represent the mean ± SD (*$p < 0.01$ by Tukey's test). (b) Western blot analysis of POT1 (left panel). Densitometry analysis of the western blot is shown in the right panel. (c, d) Control shRNA or shPot1a-1-transduced 8 week-old LSK cells were cultured for 2–4 weeks, and

colony formation was analyzed. (c) Number of CFU-Cs. (d) Number of HPP-CFCs. Data are expressed as the mean ± SD (n = 3, *p < 0.01 by *t*-test).

(e) Schematic of the analysis of cell number and apoptosis of LT-HSCs after the knockdown of Pot1a. (f) Number of total cells and LT-HSCs on day 4, 7, and 10 of culture. Data are expressed as the mean ± SD (n = 8-9, *p < 0.01 by *t*-test). (g) Percentage of Annexin V^+PI^+ apoptotic cells in LT-HSCs on day 4, 7, and 11 of culture. Data are expressed as the mean ± SD (n = 6-7, *p < 0.01 by *t*-test).

(h-j) Effects of Pot1a knockdown on HSC LTR activity. (h) Percentages of GFP^+ donor-derived ($Ly5.1^+$) cells in recipient mice peripheral blood (PB) after 4, 8, and 16 weeks BMT. Data are expressed as the mean ± SD (n = 7/group, *p < 0.01 by *t*-test) from 3 independent experiments for shPot1a-1 and -2. (i) Percentage of B cells ($B220^+$), T cells ($CD3^+$), and myeloid ($Mac\text{-}1^+/Gr\text{-}1^+$) cells in GFP^+ donor-derived cells 4 months after BMT. Data are expressed as the mean ± SD (n = 7, *p < 0.01 by *t*-test). (j) Percentage of GFP^+ donor cells in BM LSK and LT-HSCs.

(k) LT-HSCs were co-transduced with a retrovirus expressing shPot1a-1 or -2 and a retrovirus expressing control-monomeric Kusabira-Orange1 (mKO1) or smPot1a-mKO1. After retroviral transduction, LT-HSCs (control-$shRNA^+$/control-$mKO1^+$, control-$shRNA^+$/$smPot1a^+$, $shPot1a^+$/control-$mKO1^+$, and $shPot1a^+$/$smPot1a^+$) were isolated and transplanted into lethally irradiated recipient mice. Percentage of donor-derived cells in PB 4 months after BMT is shown. Data are expressed as the mean ± SD (n = 5/group, *p < 0.01 **p<0.05 by Tukey's test).

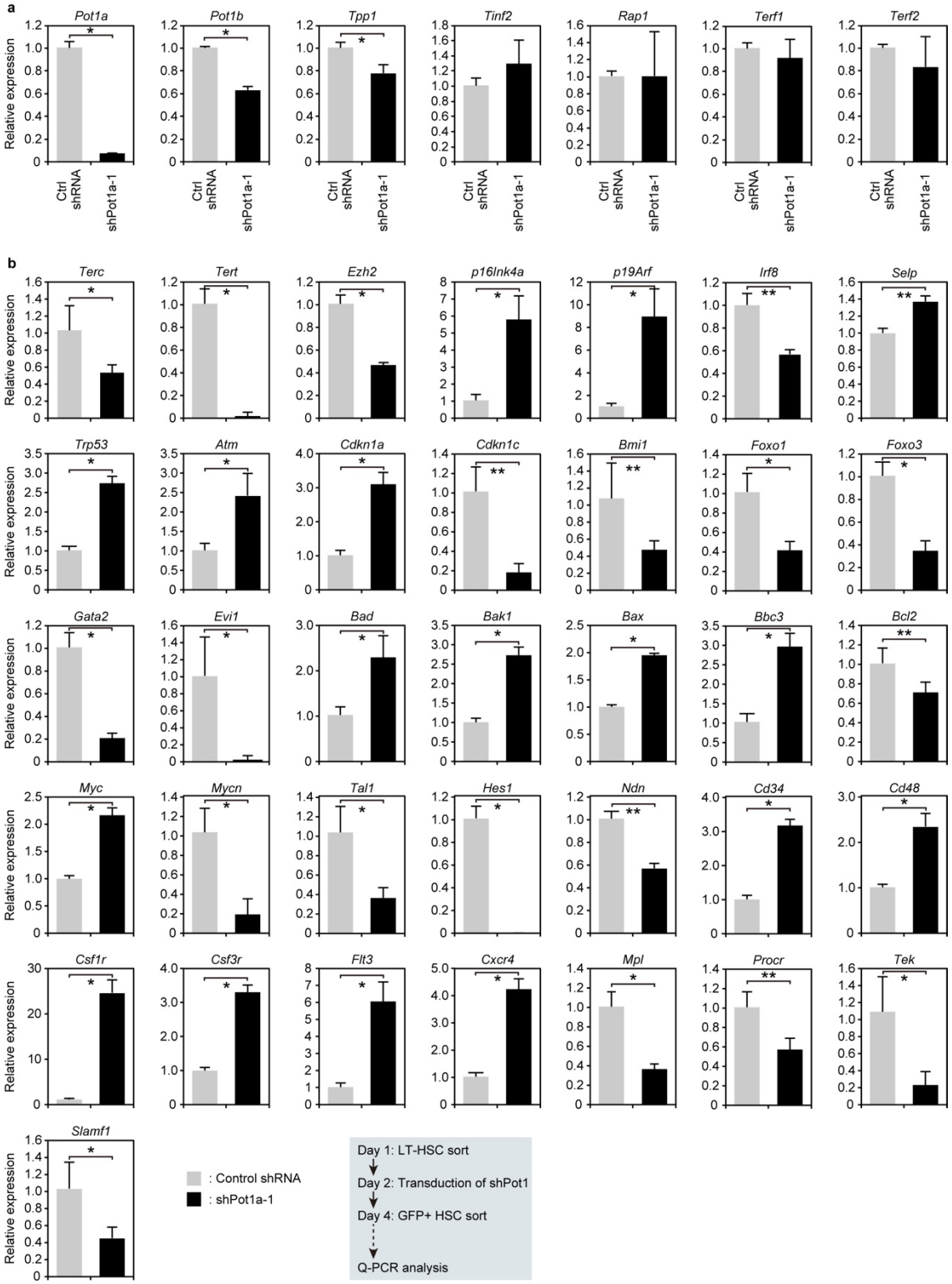

Supplementary Figure 3. Effects of *Pot1a* KD on HSC gene expression patterns.

LSKCD41^{-}CD48^{-}CD150^{+} LT-HSCs were transduced with shPot1a or control shRNA. After transduction of the shRNAs, GFP^{+} HSCs were sorted and gene expression patterns were analyzed.

(a) Expression of shelterin component genes in control shRNA or shPot1a-1 transduced HSCs. Data are expressed as the mean ± SD (n = 4, *p < 0.01 by *t*-test). (b) shPot1a-transduced cells showed significantly lower expression levels of *Tpp1*, *Tert*, and *Terc*; the anti-apoptotic gene *Bcl2*; senescence-related genes *Ezh2* and *Irf8*; cell cycle-related genes *Cdkn1c*, *Foxo1*, *Foxo3a*, *Mycn*, and *Ndn*; and significantly higher levels of the pro-apoptotic genes *Bad*, *Bak1*, *Bax*, and *Bbc3*; cell cycle/DNA damage response-related genes *Atm*, *Cdkn1a*, and *Trp53*; and senescence-related genes including *p19Arf*, *p16Ink4a*, and *Selp*. shPot1a-transduced LSK cells also showed significantly lower expression of HSC maintenance-related/marker genes, and higher expression of differentiation markers than control shRNA-transduced LSK cells. Data are expressed as the mean ± SD (n = 6, *p < 0.01, **p < 0.05 by *t*-test). The bottom right panel shows a schematic of the experimental procedure.

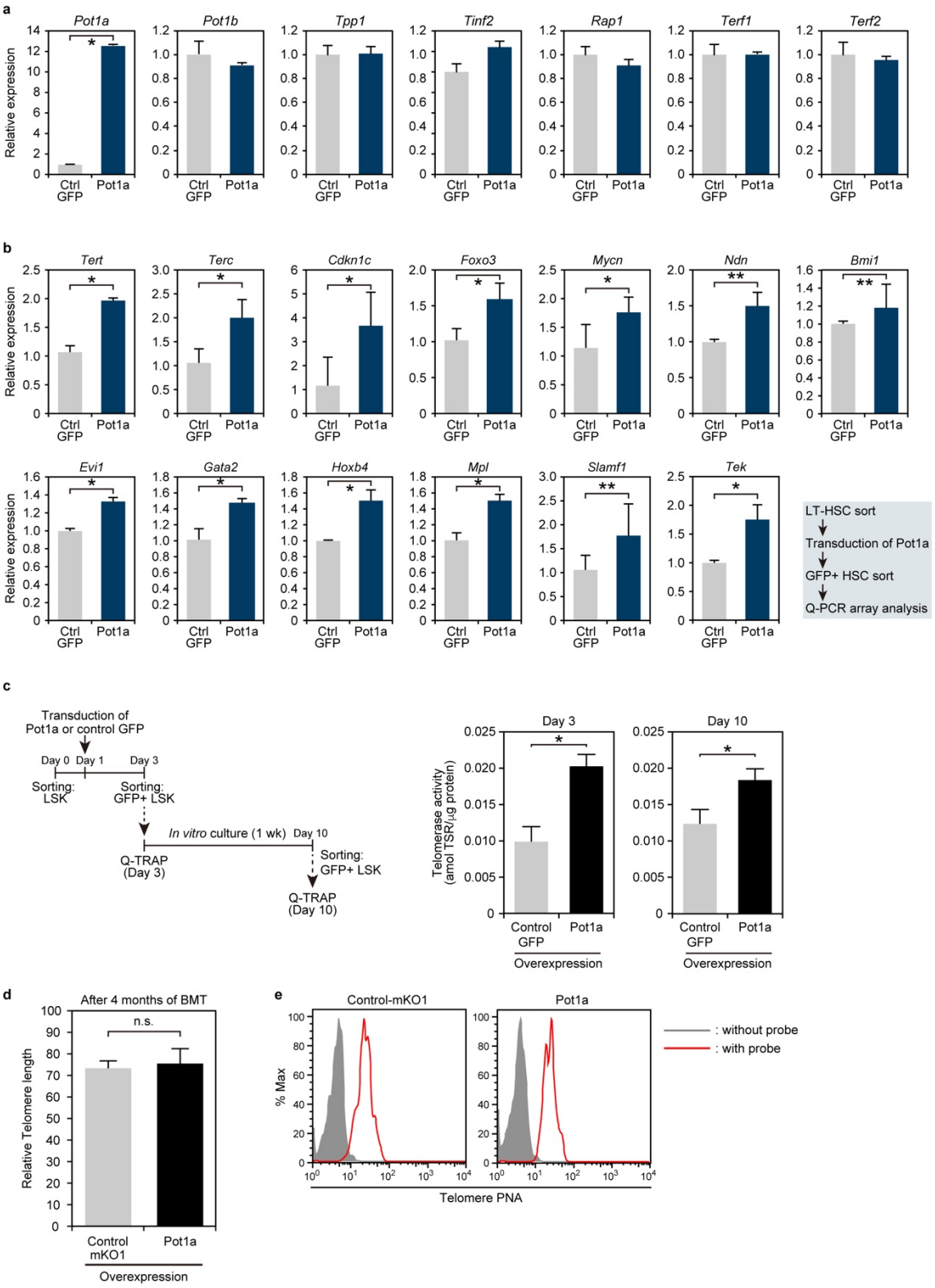

Supplementary Figure 4. Effects of Pot1a overexpression on HSC gene expression patterns and telomerase activity.

LSKCD41^{-}CD48^{-}CD150^{+} LT-HSCs were transduced with control GFP or Pot1a. After retroviral transduction, GFP^{+} LSK cells were sorted and gene expression patterns were analyzed. (a) Expression of shelterin component genes after overexpression of Pot1a. Data are expressed as the mean ± SD (n = 4, *p < 0.01 by *t*-test) (b) Overexpression of Pot1a induced the upregulation of *Tert*, *Terc*, *Cdkn1c*, *Foxo3*, *Mycn*, *Ndn*, *Bmi1*, *Evi1*, *Gata2*, *Hoxb4*, *Mpl*, *Slamf1*, and *Tek* (*Tie2*). Data are expressed as the mean ± SD (n = 6, *p < 0.01, **p < 0.05 by *t*-test). The bottom right panel shows a schematic of the experimental procedure.

(c-e) Effects of Pot1a overexpression on telomerase activity and telomere length in HSCs. (c) Schematic of the telomerase activity assay (left). LSK cells were transduced with control GFP or Pot1a. After 2 days of retroviral transduction, GFP^{+} LSK cells were sorted and telomerase activity was measured by a quantitative telomeric repeat amplification protocol (Q-TRAP) method. Simultaneously, sorted GFP^{+} LSK cells were re-cultured for 1 week. After culture, GFP^{+} LSK cells were re-isolated and the telomerase activity was measured by Q-TRAP. Results of Q-TRAP assay on day 3 and day 10 are shown in the right panels. Data are expressed as the mean ± SD (n = 4, *p < 0.01 by *t*-test). Representative data from two independent experiments are shown. (d, e) Control mKO1- or Pot1a-transduced LSK cells were transplanted into lethally irradiated recipient mice. 4 months after BMT, mKO1^{+} donor-derived LSK cells were isolated and telomere length was assessed by Flow FISH. (d) Relative telomere length. Data are expressed as the mean ± SD (n = 4, n.s., not significant by *t*-test). (e) Representative histograms of telomere PNA.

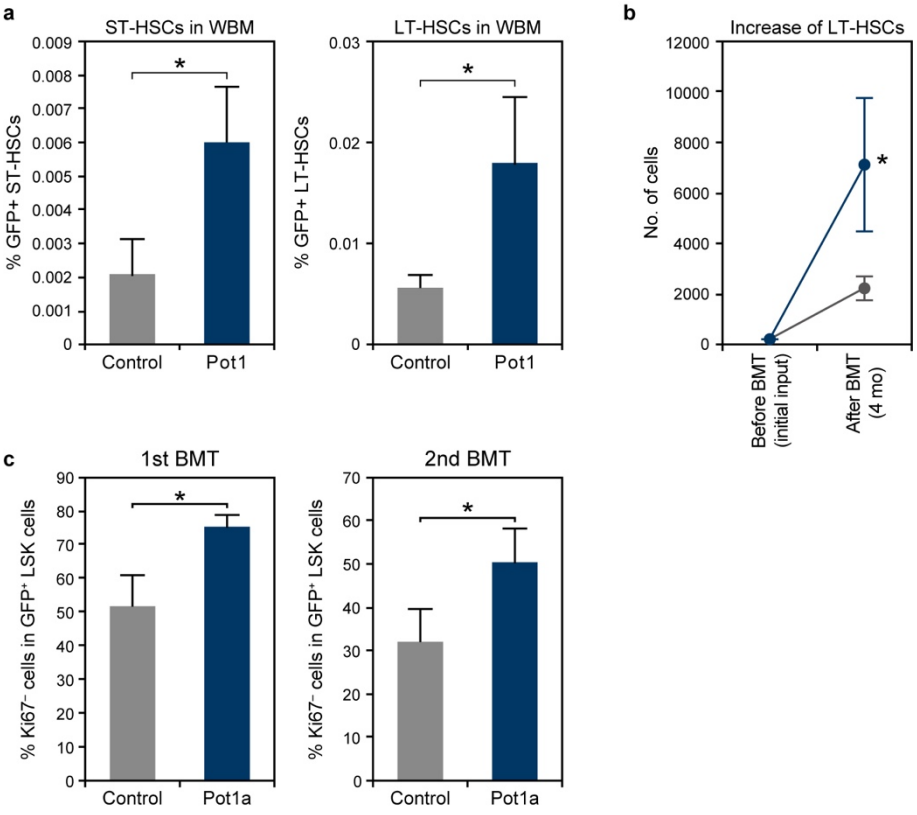

Supplementary Figure 5. Effect of Pot1a overexpression on the number and cell cycle quiescence of LT-HSCs after BMT.

(a) Control GFP or Pot1a-transduced LT-HSCs were transplanted into lethally irradiated mice (250 cells/mice). After 5 month of BMT, the percentage of donor-derived (GFP^+) ST-HSC and LT-HSC in whole BM cells (WBM) was analyzed. (b) Increase of the number of LT-HSCs after BMT. Data are expressed as the mean ± SD (n = 5, *p < 0.01 by *t*-test). Representative data from two independent experiments are shown. (c) Percentage of $Ki67^-$ cells in donor-derived (GFP^+) LSK cells after 1st and 2nd BMT. Data are expressed as the mean ± SD (n = 5: 1st BMT, n = 6: 2nd BMT, *p < 0.01 by *t*-test).

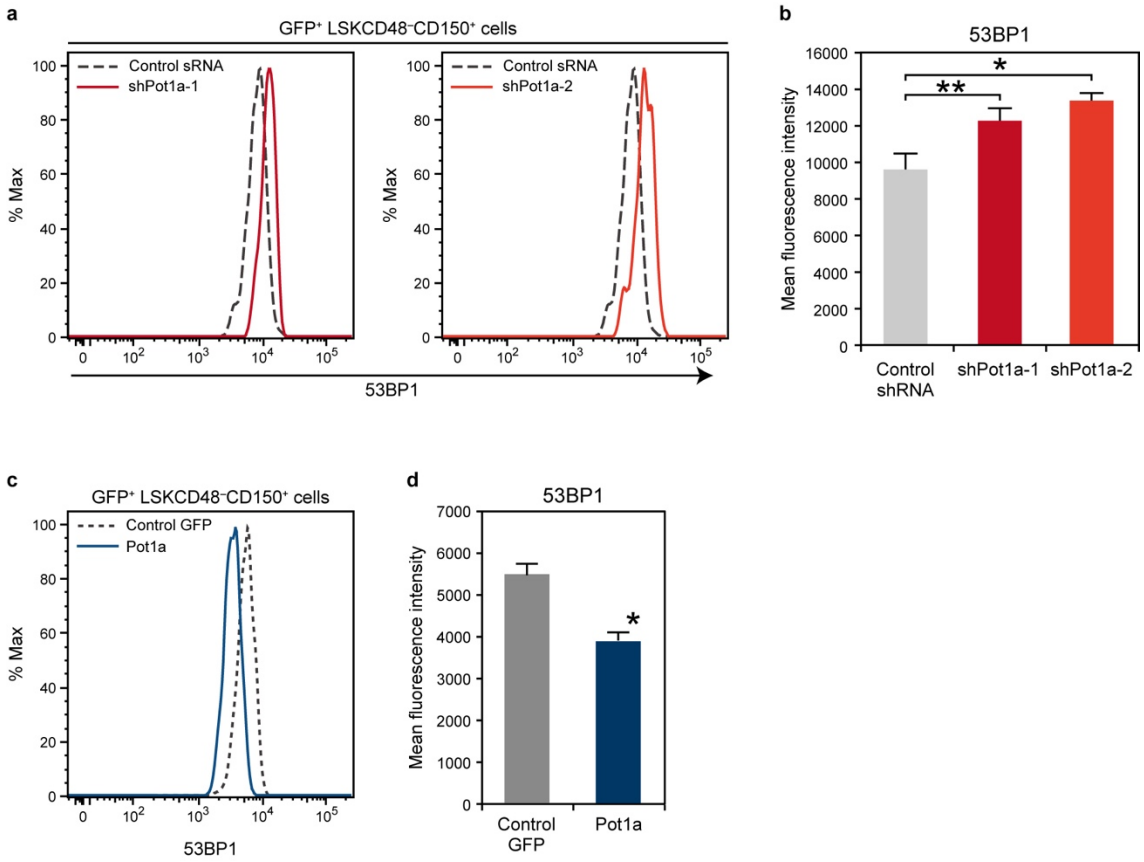

Supplementary Figure 6. 53BP1 expression level in Pot1a-overexpressing or -knockdown LT-HSCs after the culture.

(a, b) LT-HSCs were transduced with shPot1a-1, -2 or control shRNA. After 1 week of culture, 53BP1 level in GFP$^+$LT-HSC fraction was analyzed. (a) Representative FACS profiles of 53BP1. (b) Mean fluorescence intensity of 53BP1. Data are expressed as the mean ± SD (n = 5, *p < 0.01, **p < 0.05 by Tukey's test).

(c, d) LT-HSCs were transduced with Pot1a or control-GFP were cultured for 2 weeks. After the culture, 53BP1 level in gene transduced GFP$^+$LT-HSCs was analyzed. (c) Representative FACS profiles of 53BP1. (d) Mean fluorescence intensity of 53BP1. Data are expressed as the mean ± SD (n = 9, *p < 0.01 by *t*-test).

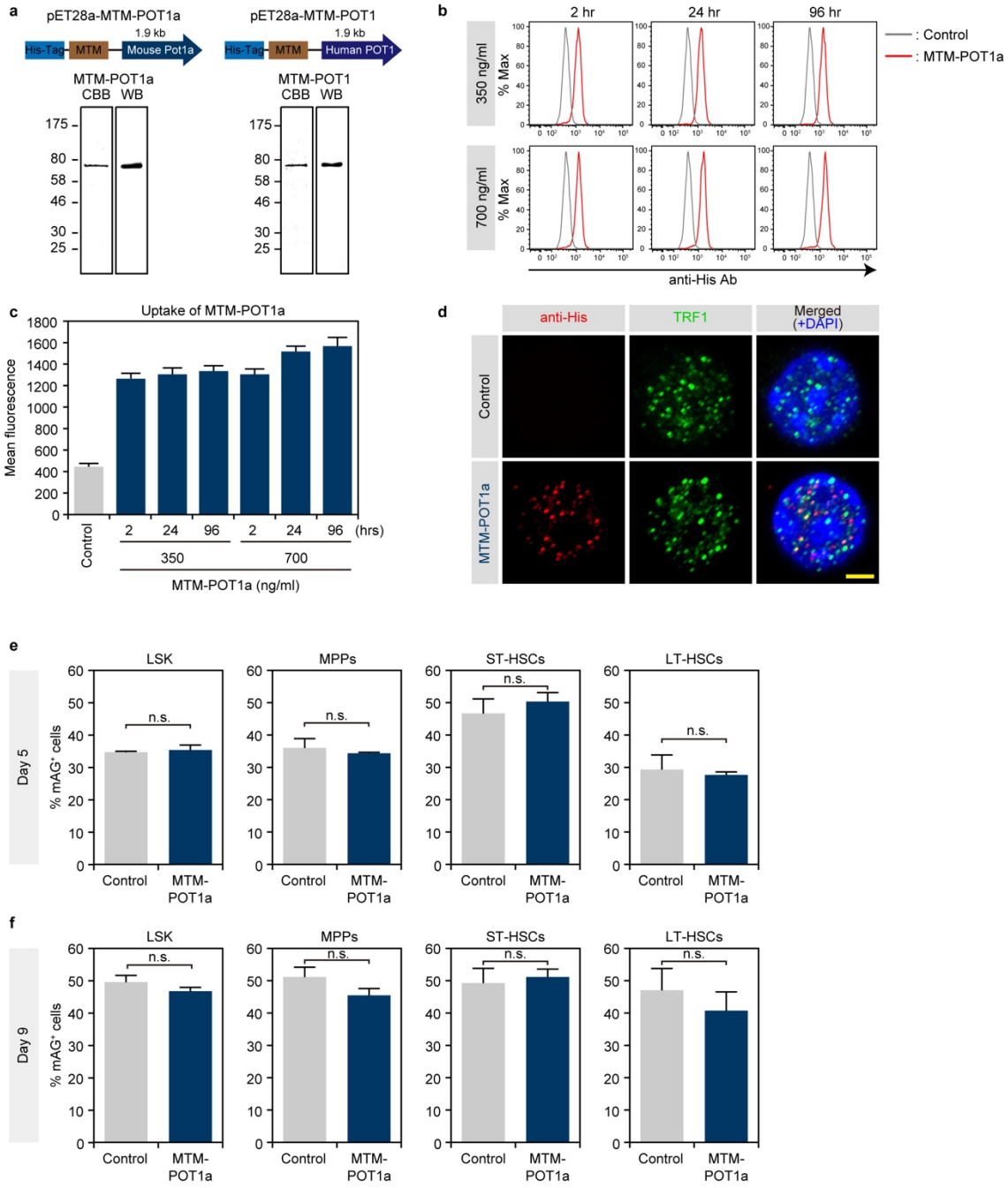

Supplementary Figure 7. Preparation of MTM-POT1a/POT1 proteins.

(a) Vector construction of pET28a-MTM-POT1a (left) and -POT1 (right). Full-length mouse Pot1a or human POT1 was inserted into the multi-cloning site (MCS) of pET28a vector which have a His- and MTM-tag at the N-terminus of MCS (upper). Purification of MTM-proteins (lower). The protein fraction was separated by sodium dodecyl sulfatepolyacrylamide gel electrophoresis and transferred to a polyvinylidene difluoride membrane following purification.

The transferred protein was detected by immunoblotting with an anti-His Ab (right), and the membrane was stained with Coomassie brilliant blue (left). The purified MTM-POT1a migrated as a single band on sodium dodecyl sulfate–polyacrylamide gels stained with Coomassie brilliant blue. The apparent mobility of the tagged protein corresponded to the expected size of 74 kDa. (b) Representative FACS profiles of anti-His staining of LT-HSCs cultured with 350 ng/ml (upper) and 700 ng/ml (lower) of MTM-POT1a. The majority of LT-HSCs incorporated MTM-POT1a within 2 hours. (c) Relative mean fluorescent intensity of LT-HSCs cultured with 350 ng/ml (upper) and 700 ng/ml (lower) of MTM-POT1a. Data are expressed as the mean ± SD (n = 3). (d) The localization of recombinant POT1a in LT-HSCs was confirmed by immunocytochemistry. LT-HSCs cultured with MTM-POT1a overnight were co-stained with anti-TRF1 (green) and anti-His-Tag (red) Abs, and the nuclei were detected by DAPI (blue). Scale bar, 2 μm.

(e, f) Function of MTM-POT1a in cell cycle progression (%S/G2/M) of HSPCs. LT-HSCs from Fucci mice were cultured for 9 days with or without MTM-POT1a (350 ng/ml). After 5 (e) and 9 (f) days of culture, the percentage of monomeric Azami-Green 1-positive (mAG^{+}) cells, corresponding to the percentage of cells in S/G2/M phase, in LSK, MPP, ST-HSC, and LT-HSC fractions was analyzed. MTM-POT1a did not affect the frequency of S/G2/M cells in any of the cultures. Data are expressed as the mean ± SD (n = 3. n.s., not significant by *t*-test).

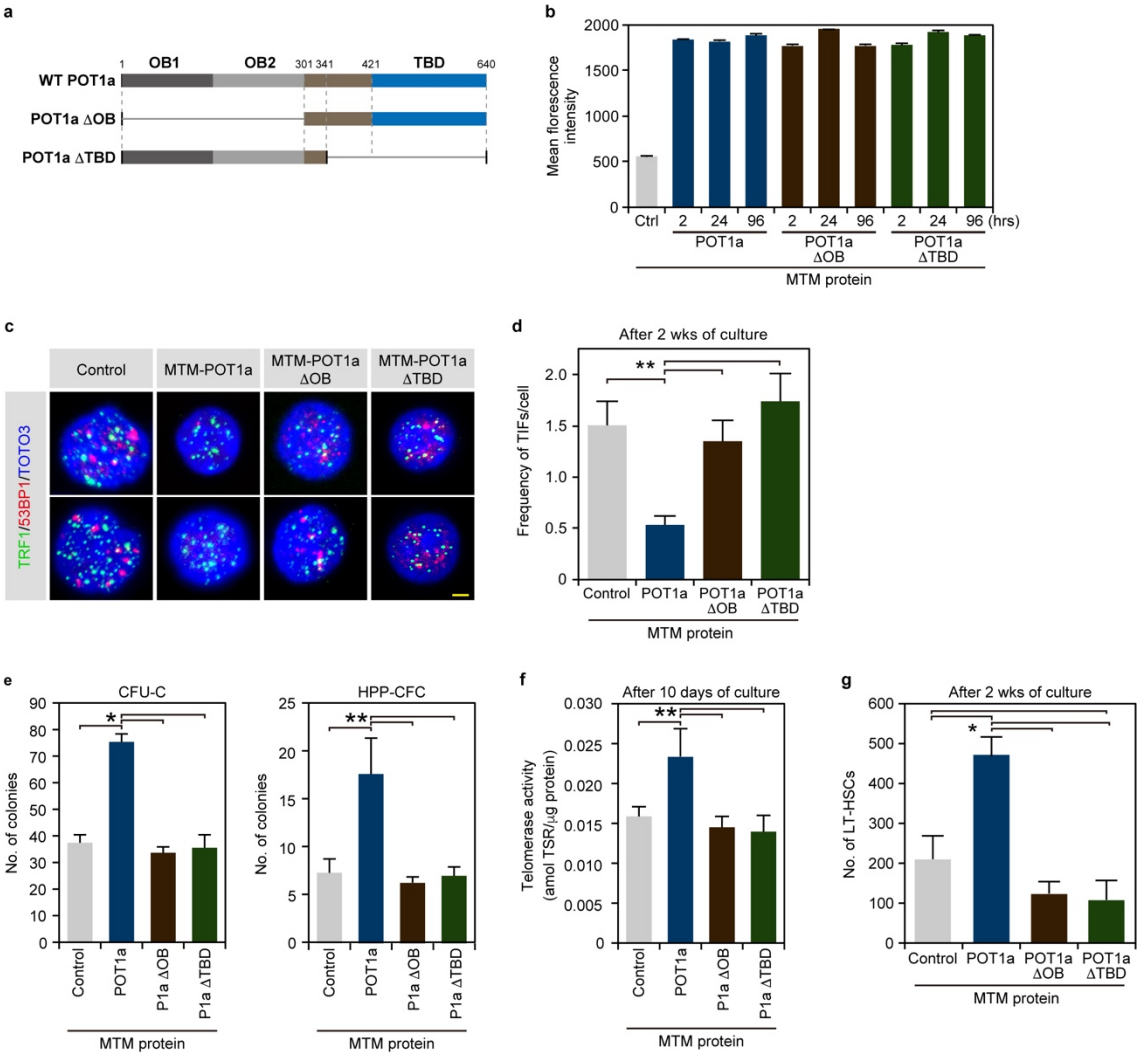

Supplementary Figure 8. Effect of mutant forms of POT1a on HSC function.

(a) Schematic of wild type (full-length) POT1a and mutant forms of POT1a lacking OB-fold domains (POT1aΔOB) or Tpp1 biding domain (TBD) (POT1aΔTBD). (b) Relative mean fluorescent intensity of LT-HSCs cultured with control MTM-protein, wild type MTM-POT1a, MTM-POT1aΔOB and MTM-POT1aΔTBD. Data are expressed as the mean ± SD (n = 3). (c, d) Effect of mutant forms of POT1a on the prevention of telomeric DDR in LT-HSCs during culture. (c) Immunocytochemical staining of TRF1 (green) and 53BP1 (red). Scale bar, 2 μm. (d) Frequencies of TIFs in LT-HSCs after 2 weeks of culture are shown. Data are expressed as the mean ± SD (n = 22-25, **p < 0.05 by Tukey's test). (e) Effect of mutant forms of POT1a MTM protein on the colony forming ability. Data are expressed as the mean ± SD (n = 3, *p < 0.01 by Tukey's test). Representative data from two independent experiments are shown. (f) Effect of wild-type and mutant forms of POT1a on the telomerase activity of LT-HSCs. LT-HSCs were

cultured for 10 days with MTM proteins and the telomerase activity was measured by Q-TRAP. Data are expressed as the mean ± SD (n = 4, *p < 0.01 by Tukey's test). Representative data from two independent experiments are shown. (g) Effect of MTM proteins on the expansion of LT-HSCs *in vitro*. LT-HSCs (200 cells/well) were cultured with MTM-POT1a or mutant forms of POT1a for 2 weeks. Numbers of LT-HSCs after culture are shown. Data are expressed as the mean ± SD (n = 4, *p < 0.01 by Tukey's test). Representative data from two independent experiments are shown.

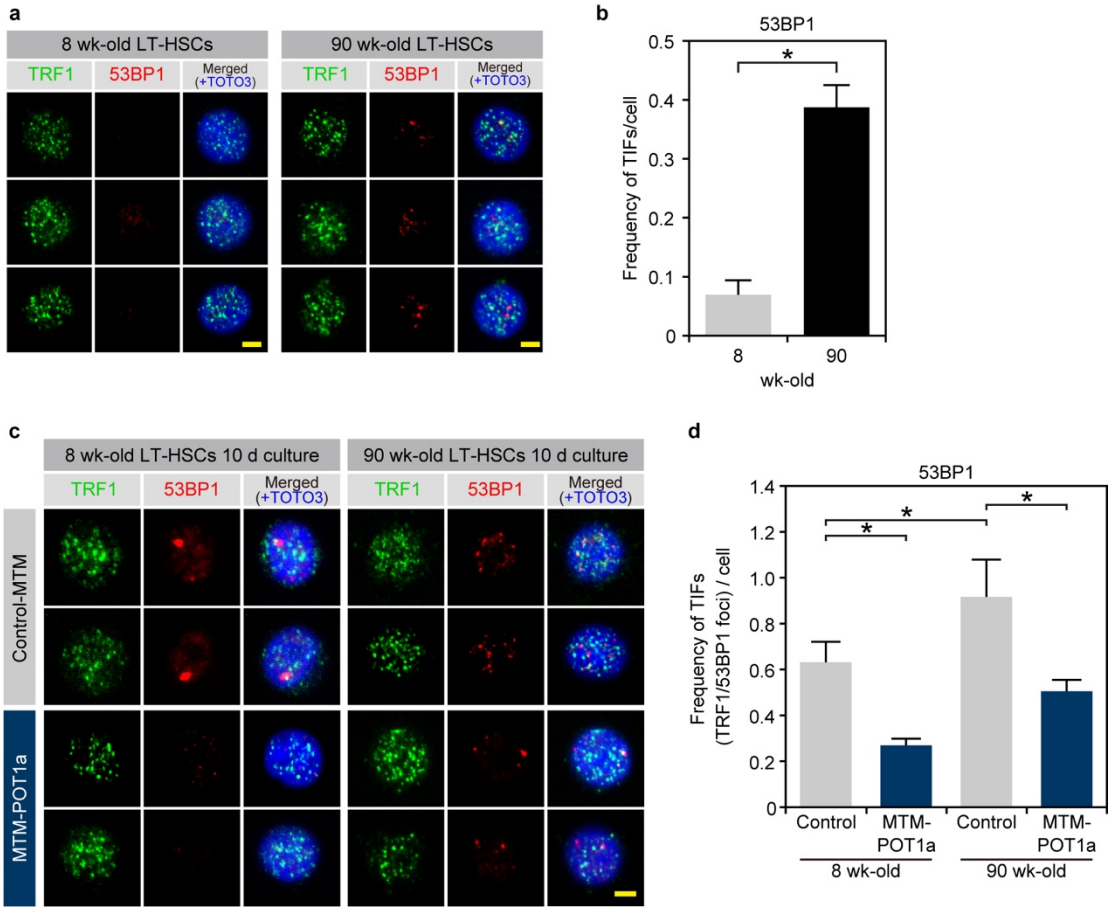

Supplementary Figure 9. Effect of MTM-POT1a on the prevention of DNA damage in aged LT-HSCs.

(a) Immunocytochemical staining of TRF1 (green) and 53BP1 (red) in LT-HSCs isolated from 8- and 90-week-old mice. Nuclei were stained with TOTO-3 (blue). Scale bar, 2 µm. (b) Frequency of TIFs per cell. Data are expressed as the mean ± SD (n = 90-100, *p < 0.01 by *t*-test). Representative data from three independent experiments are shown. (c, d) DNA damage response in LT-HSCs isolated from 8- and 90-week-old mice after *in vitro* culture. LT-HSCs were cultured for 10 days with control MTM protein or MTM-POT1a (350 ng/ml) and stained with anti-TRF1, and -53BP1 Abs. Nuclei stained with TOTO-3 (blue). (c) Immunocytochemical staining of TRF (green) and 53BP1 (red). Scale bar, 2 µm. (d) Frequency of TIFs in 8- and 90-week-old LT-HSCs after 10 days of culture. Data are expressed as the mean ± SD (n = 80–100, *p < 0.01 by Tukey's test). Representative data from 2 independent experiments are shown.

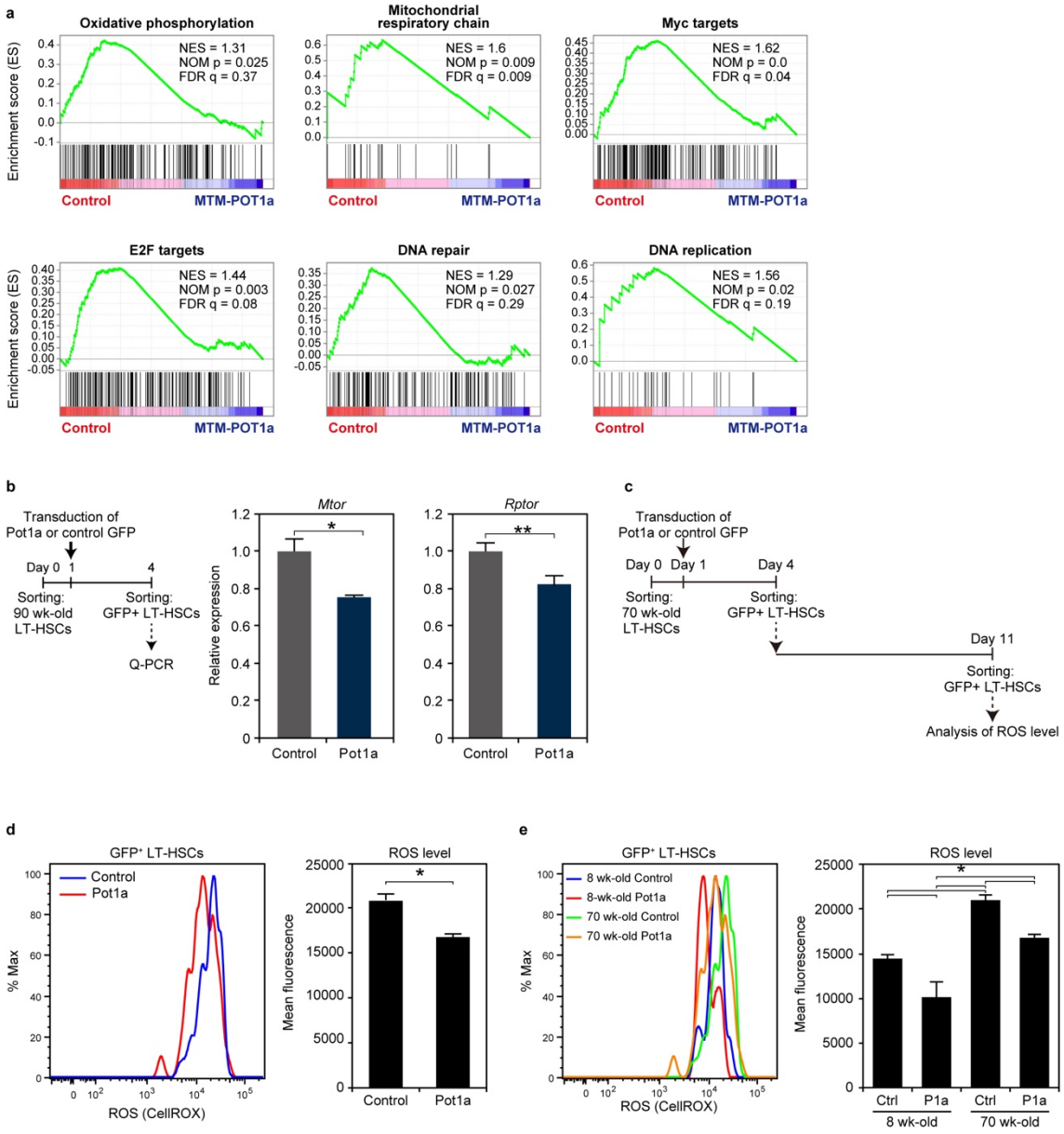

Supplementary Figure 10. Effect of exogenous Pot1a on the gene expression and ROS production in aged LT-HSCs.

(a) LT-HSCs (60 week-old) were cultured with MTM-POT1a or control MTM protein for 3 days. After the culture, gene expression profiles were analyzed by microarray. GSEA plots demonstrating enrichment levels of indicated gene sets in control MTM protein treated cells versus MTM-POT1a treated cells. NES, NOM P value, and FDR are indicated.

(b) Aged LT-HSCs (90 week-old) were transduced with control GFP or Pot1a. After 3 days post-retrovirus transduction, GFP^{+}LT-HSCs were isolated and the gene expression was examined by Q-PCR. Expression of *Mtor* and *Rptor* in Pot1a-overexpressing 90 week-old LT-HSCs was shown.

Data are expressed as the mean ± SD (n = 4, *p < 0.01 by *t*-test).

(c) Schematic of the measurement of ROS in aged LT-HSCs. Control-GFP and Pot1a-transduced LT-HSCs were cultured for 3 days. After the culture, GFP^+ LT-HSCs were isolated and re-cultured for 7 days. After the culture, intracellular ROS was measured. (d) Intracellular ROS levels in control-GFP (blue) and Pot1a-transduced (red) LT-HSCs. Representative FACS profiles of CellROX® in GFP^+ LT-HSCs were shown in left panel. Mean fluorescence level was shown in right panel. Data are expressed as the mean ± SD (n = 5, *p < 0.01 by *t*-test). (e) Comparison of ROS levels between cultured young and aged LT-HSCs that transduced with control-GFP and Pot1a. Representative FACS profiles was shown in left panel. Mean fluorescence level was shown in right panel. Data are expressed as the mean ± SD (n = 5, *p < 0.01 by Tukey's test).

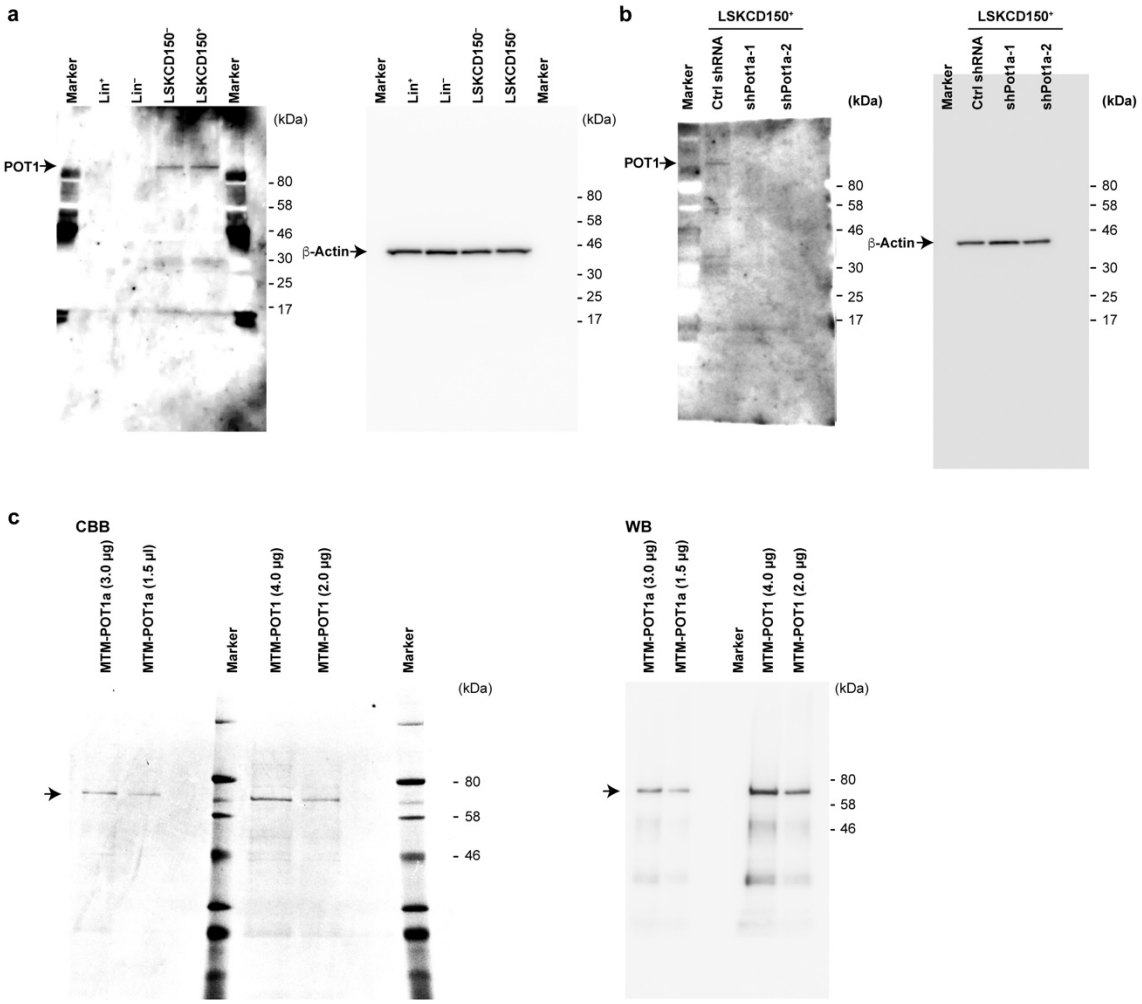

Supplementary Figure 11. Uncropped images of western blots and CBB.

(a) POT1 and β-Actin shown in Fig. 1d. (b) POT1 and β-Actin shown in Supplementary Fig. 2b. (c) CBB staining (left panel) and western blot (right panel) of MTM-POT1a/POT1 shown in Supplementary Fig. 7a.